# Learning from nature: Bio-Inspiration for damage-tolerant high-performance fibre-reinforced composites

János Plocher [a], Lorenzo Mencattelli [a,*], Federico Narducci [a] , Silvestre Pinho [a]

[a] Department of Aeronautics, Imperial College London, SW7 2AZ,

* Corresponding author: l.mencattelli@imperial.ac.uk

## ABSTRACT

Over millions of years Nature has attained highly optimized structural designs with remarkable toughness, strength, damage resistance and damage tolerance - properties that are so far difficult to combine in artificial high-performance fibre-reinforced polymers (HPFRPs). Recent studies, which have successfully replicated the structures and especially the toughening mechanisms found in flora and fauna, are reviewed in this work. At the core of the manufacturing of damage-tolerant bio-inspired composites, an understanding of the design principles and mechanisms is key. Universal and naturally-inherent design features, such as hierarchical- and organic-inorganic-structures as well as helical or fibrous arrangements of building blocks were found to promote numerous toughening mechanisms. Common to these features, the outstanding ability of diffusing damage at a sub-critical state has been identified as a powerful and effective mechanism to achieve high damage tolerance. Novel manufacturing processes suitable for HPFRP (such as tailored high-precision tape placement, micro-moulding, laser-engraving and additive manufacturing) have recently gained immense traction in the research community. This stems from the achievable and required geometrical complexity for HPFRPs and the replication of subtly balanced interaction between the material constituents. Even though trends in the literature clearly show that a bio-inspired material design philosophy is a successful strategy to design more efficient composite structures with enhanced damage tolerance and mechanical performance, Nature continues to offer new challenging opportunities yet to be explored, which could lead to a new era of HPFRP composites.

Keywords: Bio-inspired, Toughness, Composites, Damage tolerance; HPFRP;

---

TABLE OF CONTENT

# 1 Introduction

## 1.1 Promise and potential of bio-inspired composites

The requirements for today's structural materials constantly rise in pursuit of increasing strength, toughness and damage tolerance [1], [2]. These properties are however conflicting and empirical studies have shown that an improvement in either strength or toughness results in the deterioration of the opposing property, and vice versa [1]. The challenge for future materials lies therefore in the task to maintain one of the properties whilst increasing the other. Over millions of years, nature has found ways to adapt and evolve to survive under harsh environmental conditions. This led to highly optimized structures that combine unique properties [3]–[8]. Even though the building blocks of biomaterials are often quite weak [9], [10] and sometimes even orders of magnitude weaker than the whole composite, their sophisticated structure over multiple length scales allows them to combine suitable strength, toughness, stiffness, sometimes at reduced weight [1], [9]. It is exactly this potential that has driven engineers and researchers to find new ways to mimic these structures and their design principles, in order to achieve similar benchmarks in artificial bio-inspired composites [1]. This represents a challenge, since natural composites happen to be built over various scales, which implies that their properties rely on their exact configuration - all the way from structural features to the local chemical composition and their inherent mechanics [9].

According to Studart [9] and Viney et al. [11], it is essential not to simply copy these principles, but to replicate them in such a way that intrinsic attributes are met and properties are scaled with their geometry. The Ashby diagram in Figure 1 illustrates the outstanding mechanical properties of biological composites and their ability to combine toughness and high modulus.

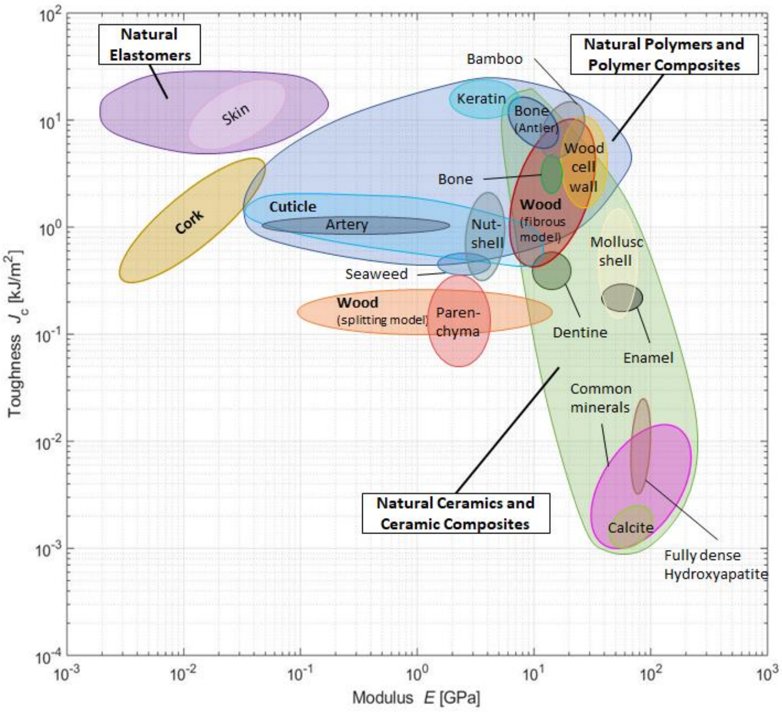


Figure 1: Ashby diagram of various natural materials, showing the relation between toughness and Young's modulus. Reproduced and adapted from [12] with permission of *Taylor&Francis*.

With the growing request for composite solutions with unprecedented structural efficiency (here simply defined as performance/weight ratio), the improvement of damage tolerance and resistance to catastrophic failure has become paramount to provide competitive composite designs. Biomimicry has therefore become an increasingly important source of inspiration for such solutions and it has seen an exponential increase since the 90's (see Figure 2). In the past, the industrial impact of bio-inspired artificial composites has been affected by the complex manufacturability of the related microstructural features, which has limited the scalability of bio-inspired composites to large structures. However, the step-change in manufacturing capabilities experienced by the composite industry in recent years opened an avenue for biomimicry to impact the industry by providing viable and competitive products that holds the potential to revolutionise conventional composite structures.

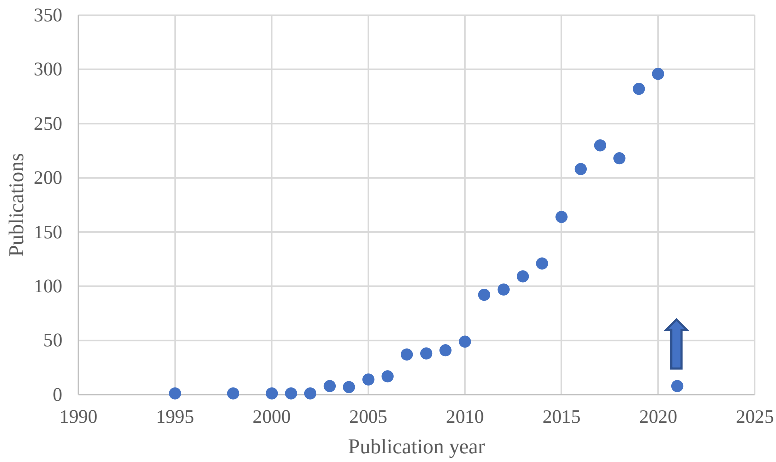


Figure 2: Exponential increase in publications related to bio-inspired composites solutions. Data obtained from Scopus using the following search parameters "TITLE-ABS-KEY (bioinspired OR biomimicry OR bio-inspired AND composites )".

This review focuses on high-performance bio-inspired fibre-reinforced composites for damage-tolerant and mechanical applications, with particular regards to the corresponding manufacturing approaches that have been successfully developed to replicate the underlying toughening mechanisms of the natural composites. Moreover, the review aims at providing a comprehensive summary of the different natural concepts that have been utilized as inspiration, the type and scale of the adopted materials used, as well as the achieved improvements in toughness and damage tolerance. Among those, this review summarises prototyped artificial bio-inspired composites and highlights the significance of high-performance fibre-reinforced polymers (HPFRPs) in this field of research. Finally, it serves as an indication and guideline for future work with respect to crucial factors that enable successful reverse engineering of tough natural composites. Figure 3 shows the organisational scheme of the present review with a schematic representing the rationale followed and the structure of each chapter.

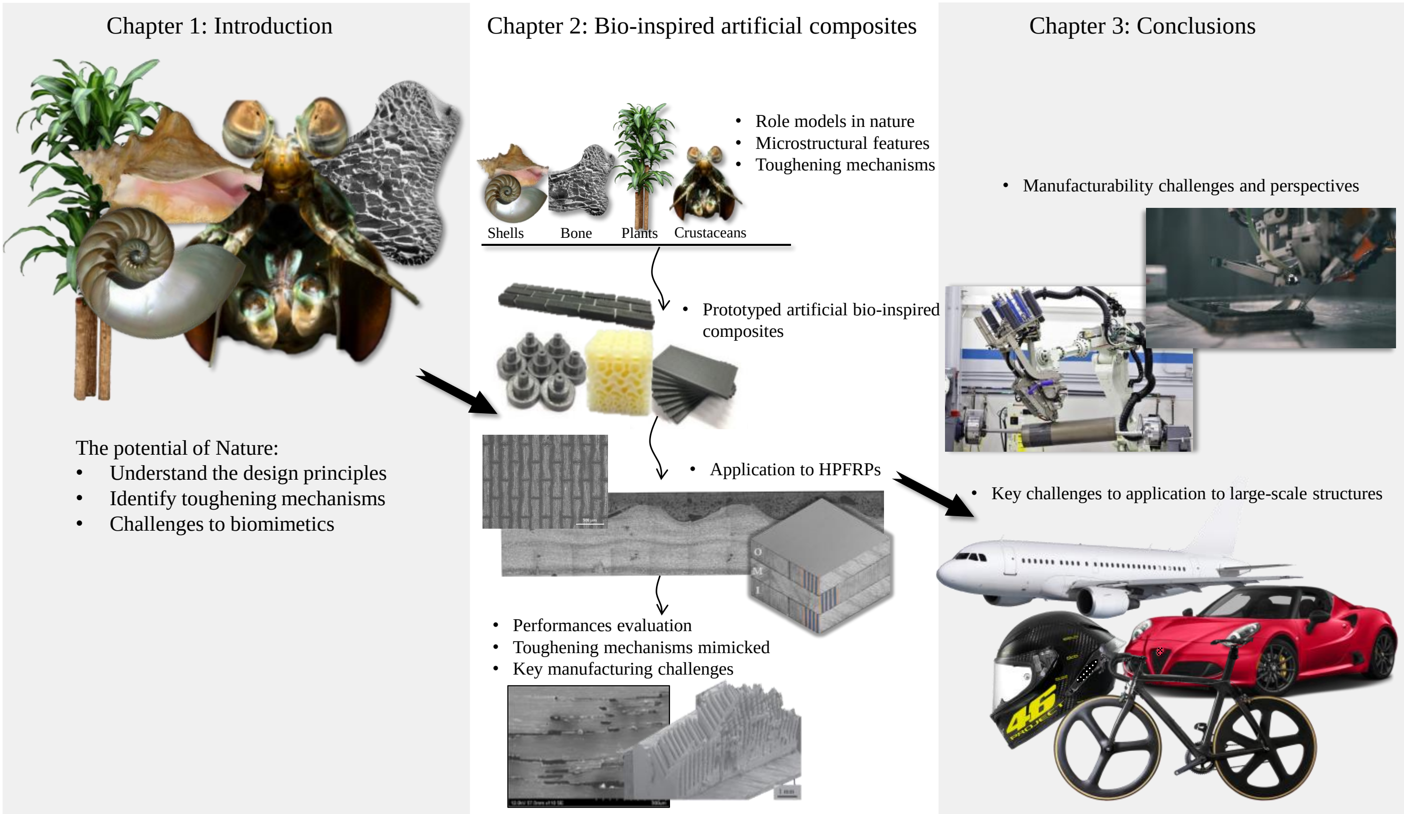


Figure 3: Organisational scheme of the present review.

## 1.2 Design principles of biological composites with high toughness

At the core of the impressive mechanical properties of bio-inspired composites are several design principles, that are built up of lesser building blocks and weak chemical bonds. Some of which have been summarised in [9] as:

- length-scale dependent geometry of building-blocks;
- building-blocks embedded in hierarchical structures;
- strong and weak bonds in a hierarchical structure (inorganic and organic constituents), i.e. inhomogeneities;
- orientation and spatial distribution of building-blocks;
- number of hierarchical levels; and
- waviness/roughness [1], [13]–[15].

Nature has found different approaches to improve the mechanical properties of its relatively weak constituents [7], [16], [17]. Nalewey et al. [18] have summarized the most important design elements that are responsible for the strong and tough nature of bio-composites. The organization of these elements on different length scales (nano- to meso-scale) results in hierarchical structures [2], [3], [7], [10], [11], [14]–[17], [19]–[57], which promote an enhanced balance of mechanical properties.

Natural composites, which incorporate the aforementioned general design principles, have proven to realize a variety of toughening mechanisms (Table 1) that can be divided into the following two categories*:* *intrinsic* toughening (resistance to crack growth initiation), which occurs at the crack tip, and *extrinsic* toughening (or shielding), which takes place in the wake of the crack tip and slows down the crack propagation [10], [17], [56], [58]. These mechanisms act at multiple length-scales, which further enhances the properties of natural composites by allowing for energy dissipation at multiple levels [1], [9], [17]. Inhomogeneity, for instance realised through the alternance of hard/soft constituents is one of the most recurrent features in natural microstructures. Inhomogeneities have been found to play a key role in providing high damage tolerance and superior strength compared to the corresponding monolithic constituents [59], [60]. An exemplification of this can be found in the deep-sea glass sponge *Monoraphis Chuni* which features a slender beam-like structure, highly subjected to bending strains. The sponge presents a cylindrical laminated structure with layers of hard silica (bio-glass) alternated to layers of soft proteins. Additionally, the thickness of the silica layers decreases from the compression to the tensile side providing tailored resistance to buckling and higher tensile strength, respectively. The laminated, i.e. inhomogeneous, nature of the microstructure leads to (i) higher resistance to crack initiation and (ii) the occurrence of crack arrest mechanisms. The latter leads to multiple crack nucleation and sub-critical damage diffusion. Compared to monolithic silica the inhomogeneous microstructure results both in higher strength (+45%) and a ten-fold increase in toughness [61], [62]. The alternance of soft/hard constituents results in a periodic variation in elastic properties which translates into a periodic variation of crack driving force, decreasing in regions with lower elastic moduli [63], [64]. Such decrease in crack driving force triggers a crack arrest mechanism which enables crack re-nucleation in the surrounding material. In a fibre reinforced structure, such a periodic change in elastic properties and hence crack driving force can be realised via periodically changing the fibre orientation such as in plywood (Bouligand-like) structures (see Section 2.5). The interaction between intrinsic and extrinsic toughening mechanisms often results in extensive sub-critical damage diffusion. Failure mechanisms, as critical as fibre failure, are controlled through diffusion, leading to stable, highly dissipative damage processes which preserve the structure from a catastrophic failure, thus resulting in outstanding damage tolerance.

Table 1: Extrinsic and intrinsic toughening mechanisms in biological composites.

| General Toughening Mechanisms | | Ref. |
|---|---|---|
| Extrinsic | Shielding/crack deflection | [1], [2], [9], [54], [56], [65]–[75] |
| | Crack bridging | [1], [56], [63], [67], [72], [76]–[78] |
| | Stretching/Tearing | [14], [57], [73] |
| | Pull-out/Interfacial hardening | [1], [13], [15], [79] |
| Intrinsic | Micro-cracking | [1], [9], [54], [80]–[82] |
| | Controlled Debonding/Sliding | [1], [13], [14], [17], [67], [68], [72], [79] |
| | Inhomogeneity | [64], [67], [68] |

### 1.3 Key challenges for biomimetic composites

A key factor for the outstanding properties of natural composites lies in the intrinsic structure of their building blocks [9]. This becomes clear when analysing the individual properties of each constituent in the composite, which are relatively weak. As shown in Figure 4, the combination of the single constituents enhances the material's overall performance beyond what would be expected from the rule of mixture. From a biomimetics viewpoint, this implies that it is crucial to pair appropriate materials for artificial composites, ensuring that they fulfil their function within the structure. Therefore, replacing a given constituent by a tougher or stronger one does not necessarily mean that the overall composite's performance will be improved [9]. Based on these challenges, Studart [9] has formulated the following tasks that need to be addressed in order to successfully reverse-engineer artificial bio-inspired composites:

- identify chemical, structural and mechanical mechanisms on each length scale;
- identify the structure-function relationship;
- incorporate the design principles of a biological composite into an artificial one.

The investigation of structure-property-functionality of biological microstructures has been central to the development of the field of biomimicry applied to artificial composites. The structure-mechanical relations of the seven hierarchical levels of bone microstructure has been analysed by Weiner and Wagner [83] to provide inspiration to the development of synthetic composite materials. Several other studies on the complex hierarchical organisation of bone [84]–[88] and tooth [89], [90] have investigated such structure-functionality relation to understand how microstructural features influence stiffness and fracture properties. An example for such structured approach applied to synthetic material can be found in a study conducted by Libonati et al. [71], in which the hierarchical bone structure was mimicked using different geometries to achieve a suitable strength-toughness balance (Figure 5).

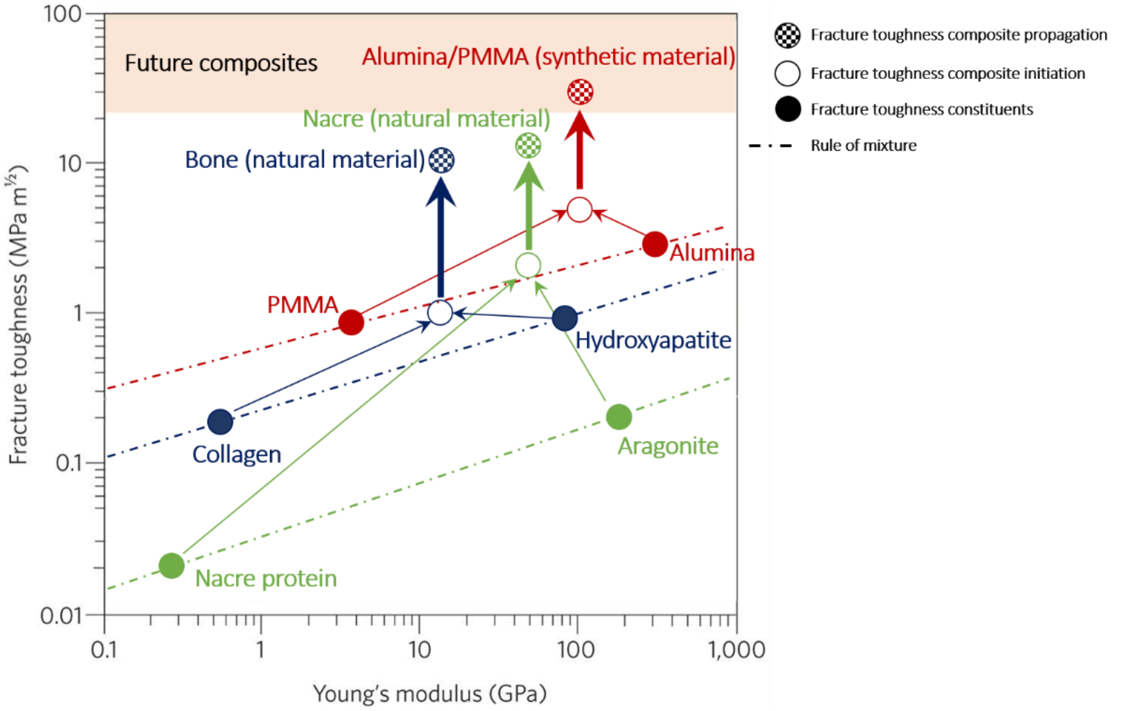


Figure 4: Compromise between toughness and Young's modulus showing several synergetic effects relative to the corresponding rule of mixtures (dashed lines) of natural constituents of nacre (green), bone (blue) and synthetic nacre inspired composite (red). The activation of extrinsic toughening mechanisms in the composite microstructures leads to value of toughness during propagation (patterned circles) larger than at crack initiation

(hollow circles). The synthetic PMMA/Alumina nacre-like composite shows similar behaviour to the natural counterpart. Reproduced and adapted from [17] with permission from *Springer*.

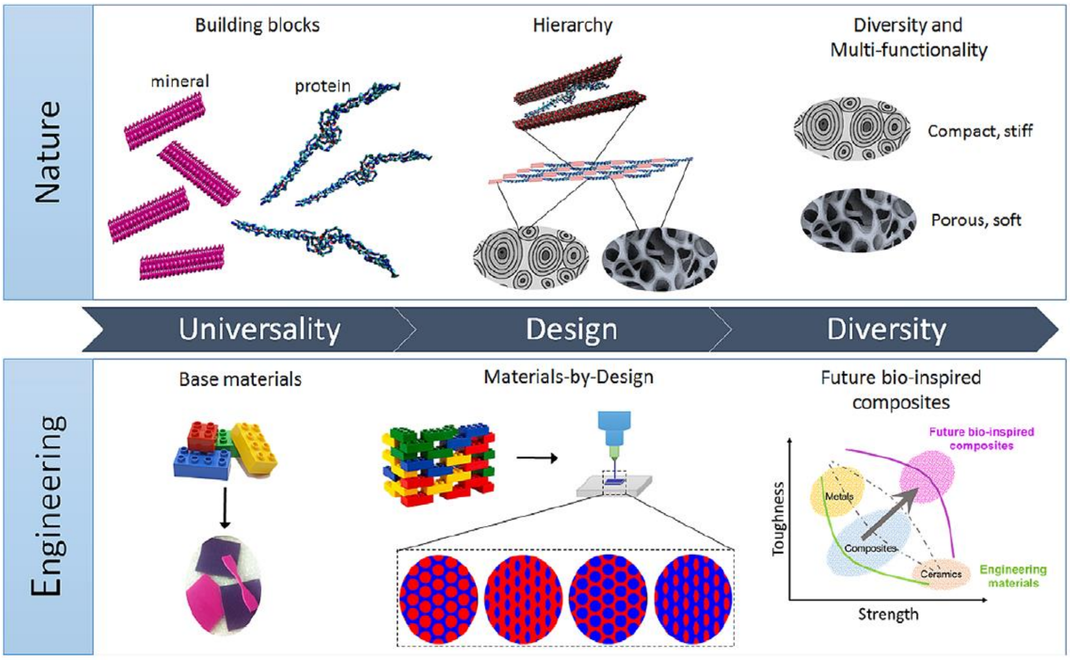


Figure 5: Mimicking bone-like hierarchical structure with additive manufacturing. Comparison between the natural and artificial approach. Reproduced from [71] with permission from *John Wiley & Sons*.

# 2 Bio-inspired artificial composites

## 2.1 Multifaceted natural role models

Effectively mimicking the fundamental structures and mechanical principles of biological composites has been the aim of intense research over recent years. In terms of improved toughness, both hard and soft tissues were investigated, revealing a broad range of inspiration from nature.

The most extensive research on hard tissues can be found on nacre-inspired materials [13], [15], [19], [25], [49], [72], [73], [80], [91]–[113], which mostly reproduce a brick-mortar structure, and on bone-inspired artificial composites [16], [33], [95], [104], [114]–[119]. Nacre can be found in the inner layer of mollusc shells [75] such as Bivalva [120], Brachiopod [53], [121] and Oyster [3], whereas research on bone-like materials also include horns or hooves [66]. Teeth [78], [81], [82], sponges [38], [61], [104], [122]–[125], plants [24], [36], [126]–[130], rhubarb [131], algae [30], [132], turtle [133], egg shell [67], snake [67], fish, clubs of crustaceans [70], [134]–[137] and the crossed-lamellar structure of the *Strombus Gigas* [138] or *Vertigastropoda* [139] have all recently been investigated for their high fracture toughness. Even though nacre in nature is not a fibrous structure, the related microstructural features offer outstanding potential for exploitation with HPFRPs to achieve enhanced toughness and damage tolerance.

In terms of soft tissues, extensive research is being carried out on silk [11], [34], [140]–[145]; in addition, the role of soft building blocks such as chitin [146]–[148] or proteins [123], [149], [150] has been investigated.

Enabling the fabrication of highly complex geometries [151] with multiple materials, Additive manufacturing (AM), specifically Inkjet processes, stand out amongst the most influential manufacturing techniques in the field to investigate features composed of hard and soft tissue [71], [115]. Numerous studies, as recently reviewed by Studart [65] and Rajasekharan et al. [152], on bio-inspired structures that are artificially reproduced using AM, reflect the strong academic effort in this field, which certainly led to an increased interest and application in the industry [153], [154]. Even preliminary studies into bio-inspired multi-functional composites, benefitting from fibre-reinforced AM, have been conducted [155]. Figure 6 displays natural design elements together with the corresponding additively manufactured samples. Often, the knowledge acquired through the investigation of AM bio-inspired microstructures has been used as initial building block for the development of similar bio-inspired concepts with HPFRPs.

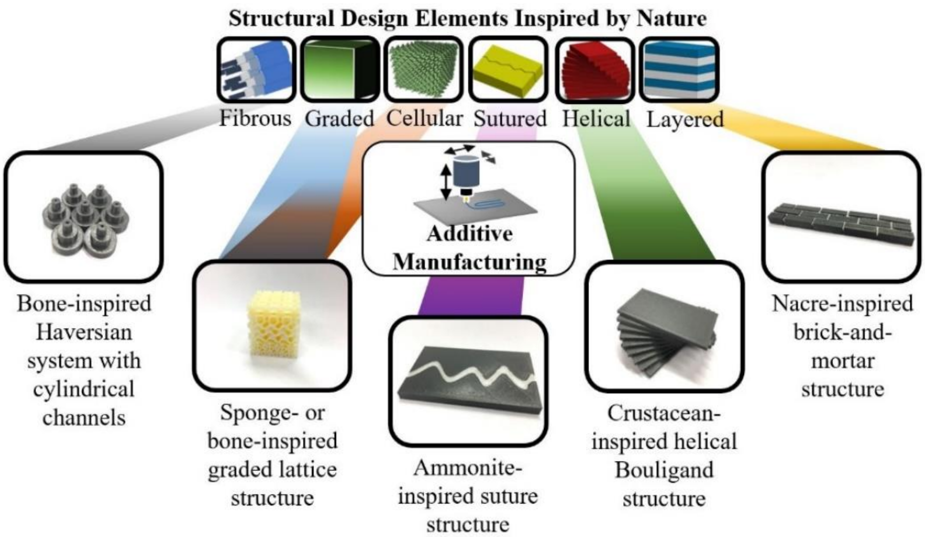


Figure 6: Nature’s core design elements as stated in [18], together with additively manufactured mock-ups.

This review focuses on hard tissues and the corresponding approaches to artificially replicate them with a specific focus on tailoring and enhancing the damage tolerance and toughness properties of HPFRPs. For the purpose of a distinct categorization, specific emphasis is put on the individual source of inspiration in nature, the possible manufacturing techniques, the materials used and the size of the reinforcement. All this is set into the context of improved damage tolerance and the mimicry of toughening mechanisms.

## 2.2 Shells

Table 2: Summary of recent studies dealing with the replication of tough bio-composites inspired to shell microstructures

| Ref | Manufacturing | Material | Scale | Performance enhancement & Toughening mechanisms |
|---|---|---|---|---|

| | | | | |
|---|---|---|---|---|
| **[156]** | • Magnetic alignment of platelets | • Reinforcement: magnetite-coated alumina platelets<br>• Matrix: polyurethane and polyvinyl-pyrrolidone | • Platelets: 7.5 µm x 200 nm | • Major improvements in mechanical properties compared to bulk material<br>• Inhomogeneities to locally control stiffness, hardness, and strength |
| **[157]** | • Vacuum assisted magnetic alignment and sintering | • Reinforcement: magnetite-coated alumina platelets<br>• Matrix: Solution of PVP and PAA | • Platelets: 7.5 µm x 200 nm | • Major increase of fracture toughness $K_{Ic}$<br>• Crack deflection and platelet pull-out |
| **[91]** | • 3D magnetic printed composites | • Reinforcement: magnetite-coated alumina platelets<br>• Matrix: Photopolymer solution | • Platelets: 7.5 µm x 350 nm | • Increased toughness due to torturous crack paths introduced by deliberate<br>• Crack deflection/twisting |
| **[158]** | • Robocasting of ceramic scaffolds, sintering and infiltration | • Reinforcement: alumina powder-platelet mix<br>• Matrix: Epoxy (Araldite resin) | • Powder (diameter 0.35 µm) and platelets (diameter 0.5 µm)<br>• Filament diameter: 100–510 µm | • Improved toughness in transverse to platelet and filament orientation<br>• Crack deflection, bridging, platelet pull-out and crack twisting |
| **[95]** | • PolyJet multi-materials 3D printing and in-situ curing | • Reinforcement: stiff photopolymer<br>• Matrix: soft, rubber-like photopolymer | • Layer-thickness: 16-30 µm | • Great energy dissipation through high damping performance<br>• Inhomogeneities provided by soft and hard component to generate high damping capability |
| **[80]** | • Multi-material 3D printing | • Reinforcement: stiff photopolymer<br>• Matrix: soft photopolymer | • Printer resolution: 16 µm | • Enhanced toughness compared to monolithic polymer<br>• Microcracking |
| **[72]** | • Freeze-casting (directional) | • Reinforcement: $Al_2O_3$-scaffold<br>• Matrix: Cyanate ester | • Lamellar $Al_2O_3$ layer: 2 µm<br>• Layer-spacing: 8 µm | • Major improvement in both toughness and strength (the former is not further quantified)<br>• Interlocking, large deformation strains, crack deflection |
| **[73]** | • Bidirectional Freezing | • Reinforcement: Hydroxyapatite (HA)<br>• Matrix: PMMA | • HA-particle: 2.424 µm (median) | • Increase in work of fracture by one to two orders of magnitude compared to monolithic HA (265 – 2075 J/m)<br>• Crack deflection, tearing and stretching, pull-out |
| **[92]** | • Freeze-casting | • Reinforcement: SiC + sinter aid $Al_2O_3$<br>• Matrix: PMMA | • Lamellar thickness: ~7.5 to ~12 µm | • Increased resistance to fracture with crack extension<br>• Crack initiation toughness of up to J~0.85kJ/m$^2$<br>• Microcracking and pull-out of SiC, stretching and tearing of PMMA |
| **[105]** | • Molded epoxy composite with partially embedded steel fibre | • Reinforcement: tapered stainless steel shaft<br>• Matrix: photocurable monomer ETPTA | • Shaft: Millimeter size | • Tapered fibre absorbs up to 27 times more energy than the straight fibre<br>• High friction coefficient increased work of pull-out<br>• Pull-out, interface hardening |
| **[108]** | • Layer-by-layer assembly with chemical bath deposition | • Reinforcement: granular $TiO_2$ film<br>• Matrix: polyelectrolyte PE | • $TiO_2$ layer: ~100 - 500 nm<br>• PE layer: ~5 - 20 nm | • Increase of toughness: up to 4 times the single $TiO_2$ layer<br>• Increase in hardness and modulus<br>• Inhomogeneity effect allows for elastic deformation of the soft constituent (PE) to delay brittle failure of the hard phase |
| **[160]** | • Laser-engraving and infiltration | • Reinforcement: borosilicate glass<br>• Matrix: PU | • Brick-size: 150 µm<br>• Interface-size: 2-2.5 µm | • 700 times tougher than monolithic glass and 10 times tougher than PE<br>• Controlled sliding of the tablets, interface hardening, strain hardening and strain rate hardening. |
| **[161]<br>[162]<br>[163]<br>[164]** | • Laser-engraved prepreg laminates | • Reinforcement: carbon-fibre glass-fibre, prepreg tiles, titanium foils<br>• Matrix: epoxy, epoxy/PLA | • Tile size: ~600 µm long, 20 µm thick | • Enhancement in volumetric energy dissipation<br>• Crack deflection, crack bridging, damage diffusion, tiles pull-out |

| | | | | |
|---|---|---|---|---|
| [165] [166] [167] | • Lamination of strips of sub-laminates with a fibre orientation of ± 45° | • Reinforcement: carbon-fibre prepreg<br>• Matrix: epoxy, PES | • 1st order lamella: 120 μm thick prepreg | • Multiple parallel cracking of first order interfaces on the tension side<br>• Crack deflection in middle layer (±45°)<br>• Frictional sliding and pull-out of lamellae in middle layer |

### 2.2.1 Microstructure of Strombus Gigas Shells

Mollusk shells, such as the *Strombus Gigas* (see Figure 7a), have an extraordinary high toughness due to their cross-lamellar structure, which is built up of calcium carbonate (99.9 wt.%) and an interstitial protein (0.1 wt.%) [168] over five length scales [48], [138] (see Figure 7b). The distinctive feature of the *Strombus Gigas* shell lies in its middle layer, consisting of three orders of lamellae, ranging from 0°/90° to alternating +45° and -45°. This layer is wedged in between the outer-layers with first order lamellae in 0°/90° [169]. As reported in Figure 7c, the major toughening mechanisms in cross-lamellar microstructures are [7]:

(i) the formation of multiple tunnelling cracks forming on the inner layer of the microstructure (tension side). These cracks tend to arrest as they approach the interface between inner and middle layer;

(ii) crack deflection at the interface with the middle layer; and

(iii) several sub-critical dissipative mechanisms activating in the middle layer including: bridging of lamellae, frictional sliding and debonding.

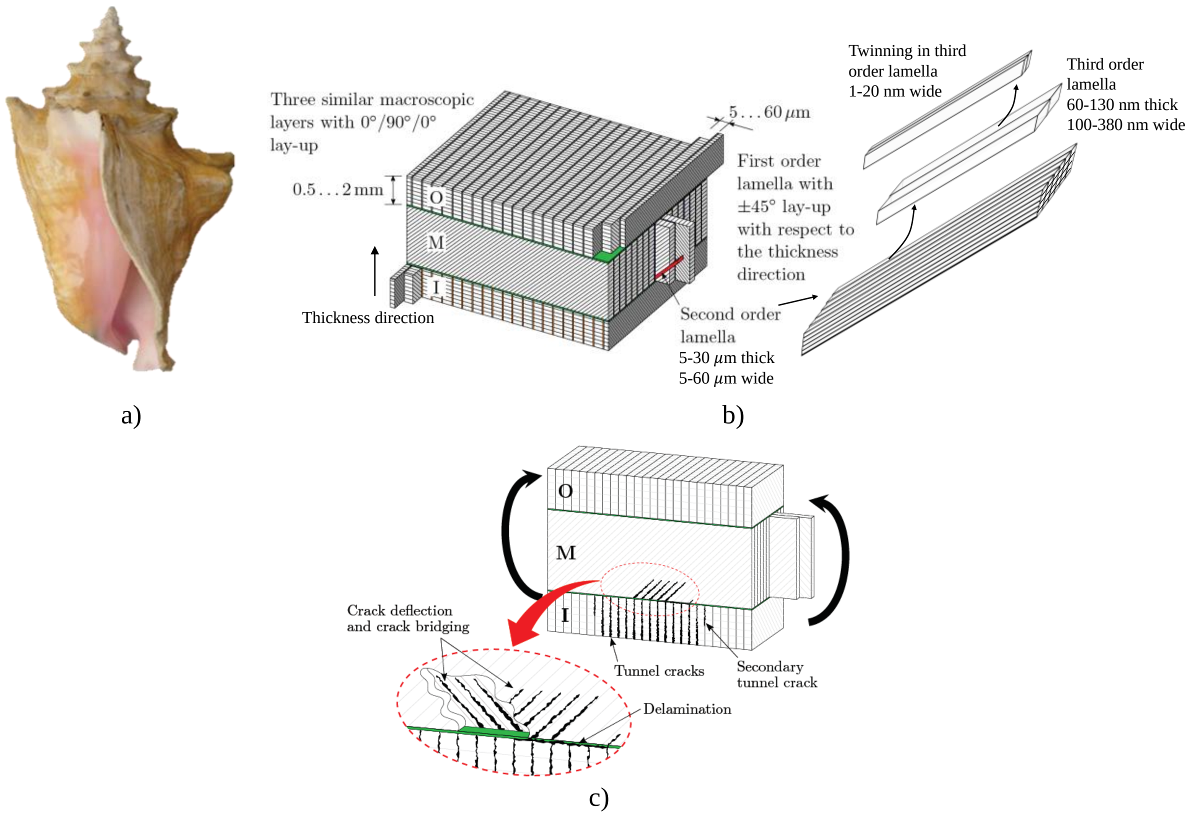

Figure 7: a) Shell of Strombus Gigas. Reproduced from [170] under the Creative Common licence. b) Crossed-lamellar microstructure and c) toughening mechanisms in cross-lamellar microstructure including: tunnelling cracks in the inner layer and consequent crack arrest at the interface with the middle layer, crack deflection in the middle layer and bridging and sliding of lamellae in the middle layer. Reproduced from [165] with permission from *Elsevier*.

#### 2.2.2 Microstructure of Nacre-like shells

Nacre is found in  the inner layer of most mollusc shells and is composed of a mineralized brick-mortar micro-structure, consisting of 95 wt.% aragonite ($CaCO_3$) platelets (or tiles) and 5 wt% organic materials, which act as a glue between the tiles [21]. The hierarchical structure of nacre (Figure 8) spans from the nano- to the macro-scale [50], [171]–[173], forming either an abalone-like columnar structure or an oyster-like sheet structure [174]. The organic-inorganic interface plays thereby an important role in the toughness of nacre, since the platelets provide the stiffness, whereas the proteins dissipate the energy and distribute it over a greater area [13]. In order for the toughening mechanisms (based on tile pull-out) to be effective, the aspect ratio of tiles (length/thickness ratio) has to be such that tiles do not fail in tension [42]. If the aspect ratio is below a certain threshold value, then tiles can be pulled out without breaking, thus leading to extensive toughening and diffusion of damage [9], [42].

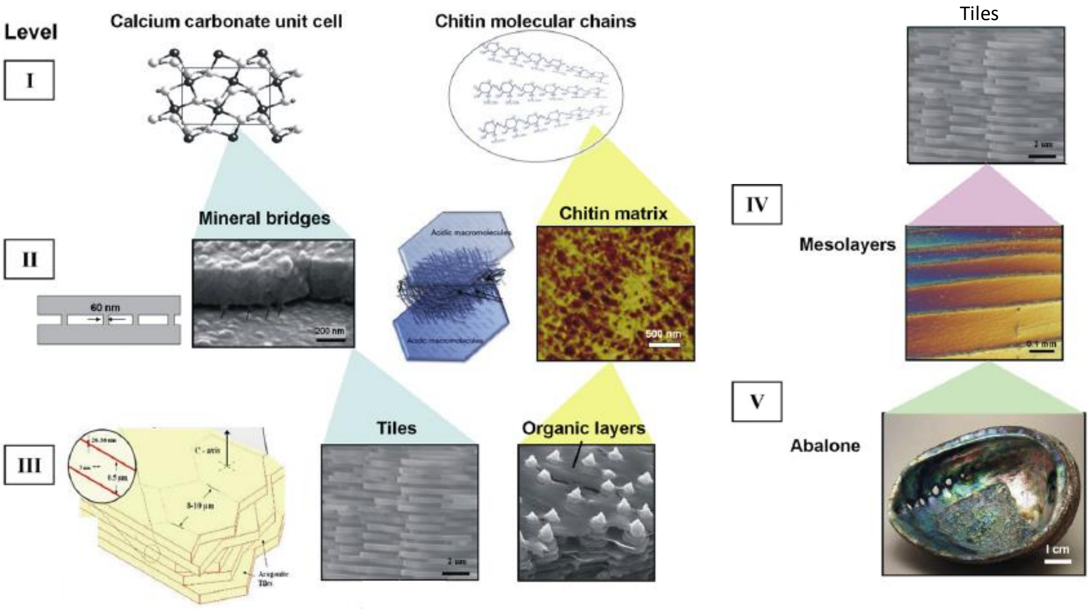


Figure 8: Nacre’s hierarchical structure over various length scales. Reproduced from [173] with permission from *Elsevier*.

#### 2.2.3 Shell-inspired artificial composite

##### 2.2.3.1 Strombus Gigas shell-inspired HPFRPs

The extraordinary damage tolerance and structural integrity shown by the cross-lamellar microstructure are very desirable features to mimic with HPFRPs. Häsä and Pinho [165] prototyped CFRP cross-lamellar microstructures using two different manufacturing procedures, namely co-cured and co-bonded (Figure 9a). The former consists in manufacturing the individual ±45° lamellae, which were laid up and cut into 2 mm wide strips. The sub-laminates were then stacked and rotated, thus creating the three main layers (inner, middle and outer). The latter consists in manufacturing each layer (inner, middle and outer) individually. Once cured, each layer was cut, rotated and re-bonded to achieve the cross-lamellar microstructure. Micrographs of the prototyped microstructures reported in Figure 9b and Figure 9c for co-cured and co-bonded procedures show that the former resulted in a better alignment and a more regular cross-lamellar microstructure.

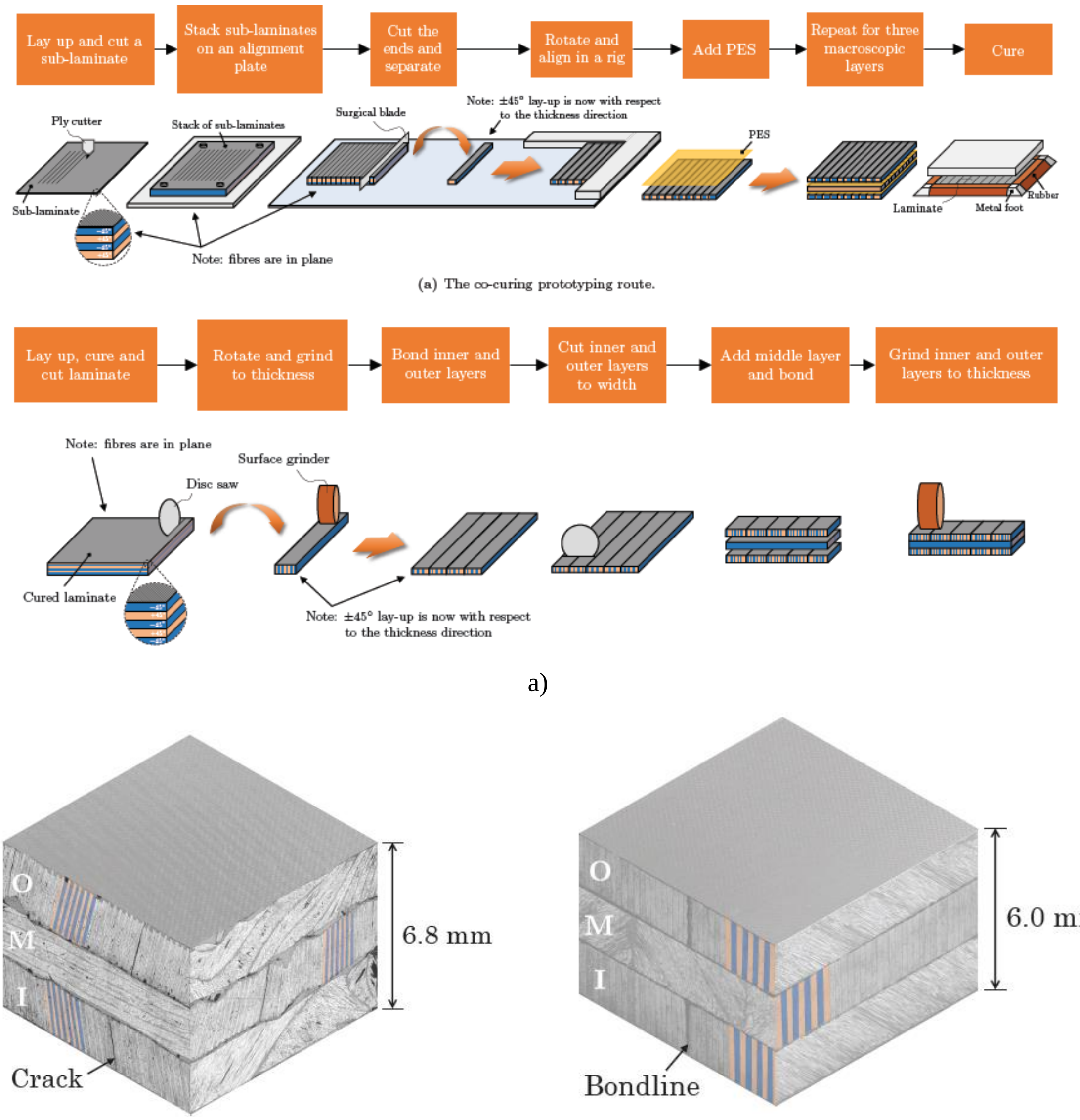


Figure 9: a) Sketch of the process followed to synthesise a Strombus Gigas-inspired CFRP: co-cured and co-bonded. Optical micro-graph of the carbon/epoxy cross-lamellar micro-structure: b) co-cured and c) co-bonded. Reproduced from [165] with permission from *Elsevier*.

Three-point bending (3PB) tests conducted in a SEM environment showed that tunnel cracks (Figure 10a) and crack deflection (Figure 10b) mechanisms were successfully achieved in the bio-inspired CFRP composites. Crack deflection mechanisms hereby led to the formation of regular pattern of matrix splits in the middle layer (Figure 10c). These sub-critical failure mechanisms contributed to a stable energy dissipation resulting in large applied displacements sustained by the structure with increasing or constant applied load (Figure 10d).

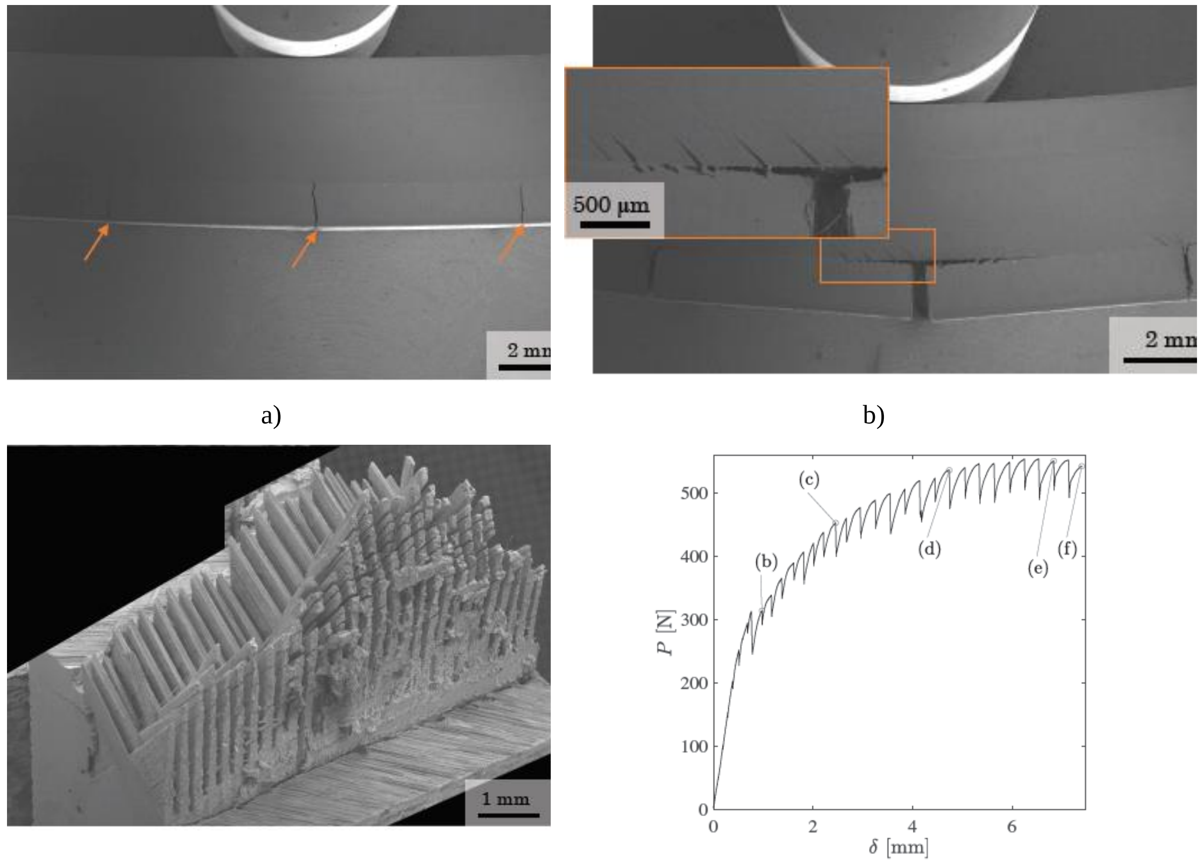


a) b)

c) d)

Figure 10: SEM images CFRP co-bonded microstructures under 3PB highlighting a) tunnel cracks in the inner layer, b) crack deflection in the middle layer and c) regular splitting in the middle layer. d) load displacement curve of the CFRP co-bonded cross-lamellar microstructure highlighting a stable mechanical response. Reproduced from [165] with permission from *Elsevier*.

Aiming at further improving the integrity of HPFRP cross-lamellar microstructures, Häsä and Pinho [166], [167] developed hybrid metal/CFRP laminates with the inner and outer layer of the microstructure made of metal (Aluminium [167] and Titanium [166]) and the middle layer, where the majority of the toughening mechanisms typical of cross-lamellar microstructures occur, made of CFRP. 3PB tests in a SEM environment revealed that the presence of the two metal layers promoted the formation of additional failure mechanisms in the middle layer including fibre kinking, diffused fibre failure and splits along the fibre thus further enhancing the energy dissipation capability of full-CFRP cross-lamellar microstructures [167]. Large scale four point bending tests of the metal hybrid laminates showed an extraordinary structural integrity with the hybrid laminates reaching large deflections without incurring into catastrophic failure, as reported in Figure 11 [166].

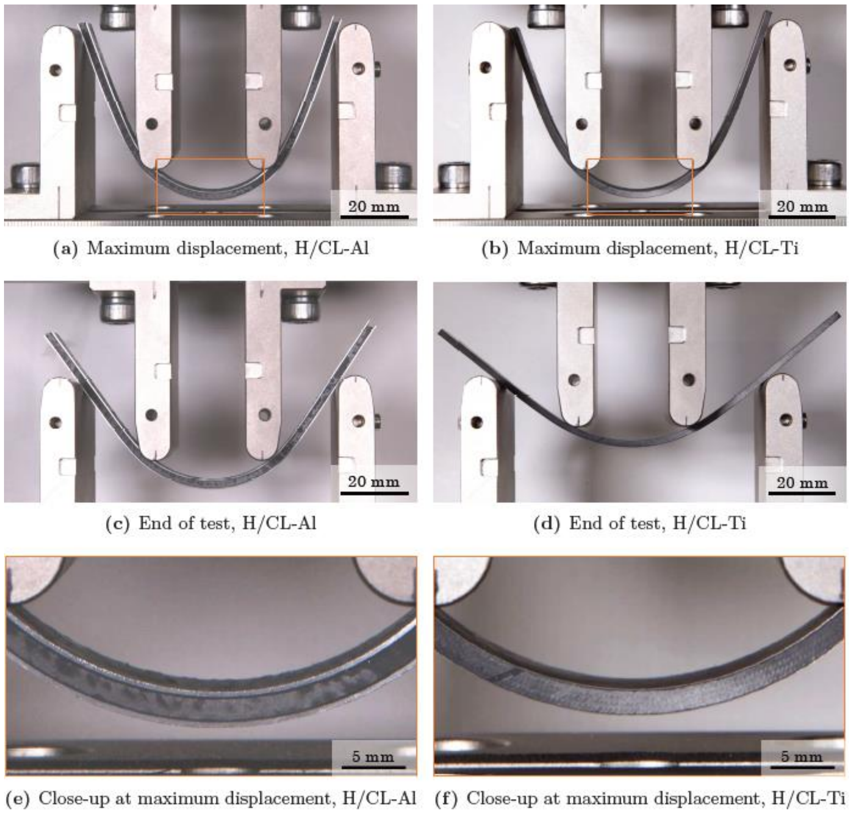


Figure 11: Snapshots during the 3PB-test of H/CL-Al (hybrid cross-lamellar with Aluminium) and H/CL-Ti (hybrid cross-lamellar with Titanium), highlighting the high structural integrity of the bio-inspired microstructures which did not fail catastrophically even at large applied displacements. Reproduced from [166] with permission from *Elsevier*.

Overall, Strombus Gigas shell inspired HPFRPs successfully mimicked the key toughening mechanisms observed in the natural microstructure, hence showing great potential for enhancing the damage resistance of conventional HPFRPs. Yet, due to the complexity related to the manufacturing process, these bio-inspired microstructures are currently limited to small prototypes. Such limitations are particularly relevant for standard hand-layup manufacturing as exemplified by the complex procedures characterised by the several steps shown in Figure 7a. The main difficulty in the mimicking of the microstructural features of the Strombus Giga's shell arises from the necessity of creating a laminated structure where the fibrous layers are perpendicular (or at an angle) with respect to the main lamination plane. The advent of high precision 3D printing of continuous HPFRPs and Continuous Fibre Manufacturing (CFM) creates an important avenue for the exploitation of such damage tolerance microstructure within larger scale components.

#### 2.2.3.2 Prototyped Nacre-inspired artificial composites

Nacre-inspired artificial composites have been prototyped with several innovative techniques and a wide variety of materials. These include alumina-reinforced polymers with tuned (magnetic field driven) orientations [156], [157], freeze-casted/Ice-Templated nacre-inspired scaffolds [72], [73], [92] and moulded steel/epoxy composites [105], electrophoretic deposition [108], [159], [175]–[178]. Several nacre-inspired artificial composites have been prototyped with additive manufacturing techniques. These include traditional 3D printing [80], Multimaterial Magnetically-assisted 3D Printing (MM-3D printing) [91], Magnetically-Assisted Slip Casting (MASC) and Robocasting [158] in addition to other processes such as PolyJet 3D printing [95], [115], Direct Ink Writing [128]. Other nacre-inspired microstructures have been created in brittle borosilicate-glass by means of a laser-engraving technique [160], [179]. Comprehensive reviews on the prototyping of nacre-inspired artificial composites can be found in [21], [180].

#### 2.2.3.3 Nacre-inspired HPFRPs

The toughening mechanisms occurring in biological nacre-like structures presented in Section 2.2.1 and explored with several prototyped artificial microstructures reported in Section 0, offer an outstanding opportunity to tackle the inherent brittleness and consequent poor damage tolerance of high-performance fibre reinforced composites, and specifically, of carbon fibre reinforced composite (CFRP) materials.

Numerous works in the literature have attempted to exploit nacre-like microstructures to achieve pseudo-ductility with CFRPs aiming at avoiding catastrophic failure [181]–[186]. The majority of works on nacre-like CFRPs has attempted to mimic the failure mechanisms observed in nacre structures found in nature (e.g. crack deflection and damage diffusion) to achieve a stable and diffused failure process, which would have been otherwise highly localised and unstable in a conventional CFRP structure. Therefore, while quantitative measures of fracture toughness are not reported in the literature, the qualitative observation of such toughening mechanisms exemplifies the enhancement in volumetric energy dissipation (high damage diffusion) of nacre-like CFRPs. Pimenta and Robinson [182] developed an analytical model to investigate the tensile response of tiled FRP composites based on different constitutive laws of the tile interface. Czel et al. [183], [184] introduced discontinuities along the load-carrying fibres of unidirectional carbon/glass laminates in order to achieve a gradual failure response. Malkin et al. [181] developed a nacre-inspired CFRP composite by introducing patterns of resin pockets aiming at creating a distribution of discontinuities mimicking a tiled nacre microstructure. Test results showed that the larger the size of the inclusion the more stable the failure response of the laminate.

Narducci et al. [161]–[163] developed a high-accuracy prototyping procedure to manufacture nacre-inspired CFRP composites with a micro-level precision by using a laser-engraving technique on uncured prepreg CFRPs (Figure 12a). Analytical models were developed to predict the energy dissipation and crack deflection capability depending on the tile geometry. Suitable geometrical parameters of interlocking tiles (approximately 600 μm in length) were selected for manufacturing. In-situ three-point bending tests conducted in a SEM environment showed that the interlocking tile geometry was capable of substantial crack deflection. Specifically, a crack formed on the tensile side of the sample and gradually propagated towards the bulk of the laminate in a 'zig-zag' type of pattern leading to a stable failure process (Figure 12b-c) [161].

Aiming at further increasing the damage tolerance of nacre-inspired CFRPs, Narducci et al. [163] investigated strategies to enhance damage diffusion by increasing the toughness of the interface between tiles. A thin layer of poly(lactic acid) (PLA) was interleaved in between

CFRP plies using a film-casting technique. The thermoplastic material was placed both as a continuous film and as fractal-shaped patches (Figure 12d). The fractal patches demonstrated to successfully promote damage diffusion of the CFRP tiles while preserving the interface strength, therefore mimicking some of the toughening mechanisms of naturally-occurring nacre-like microstructures.

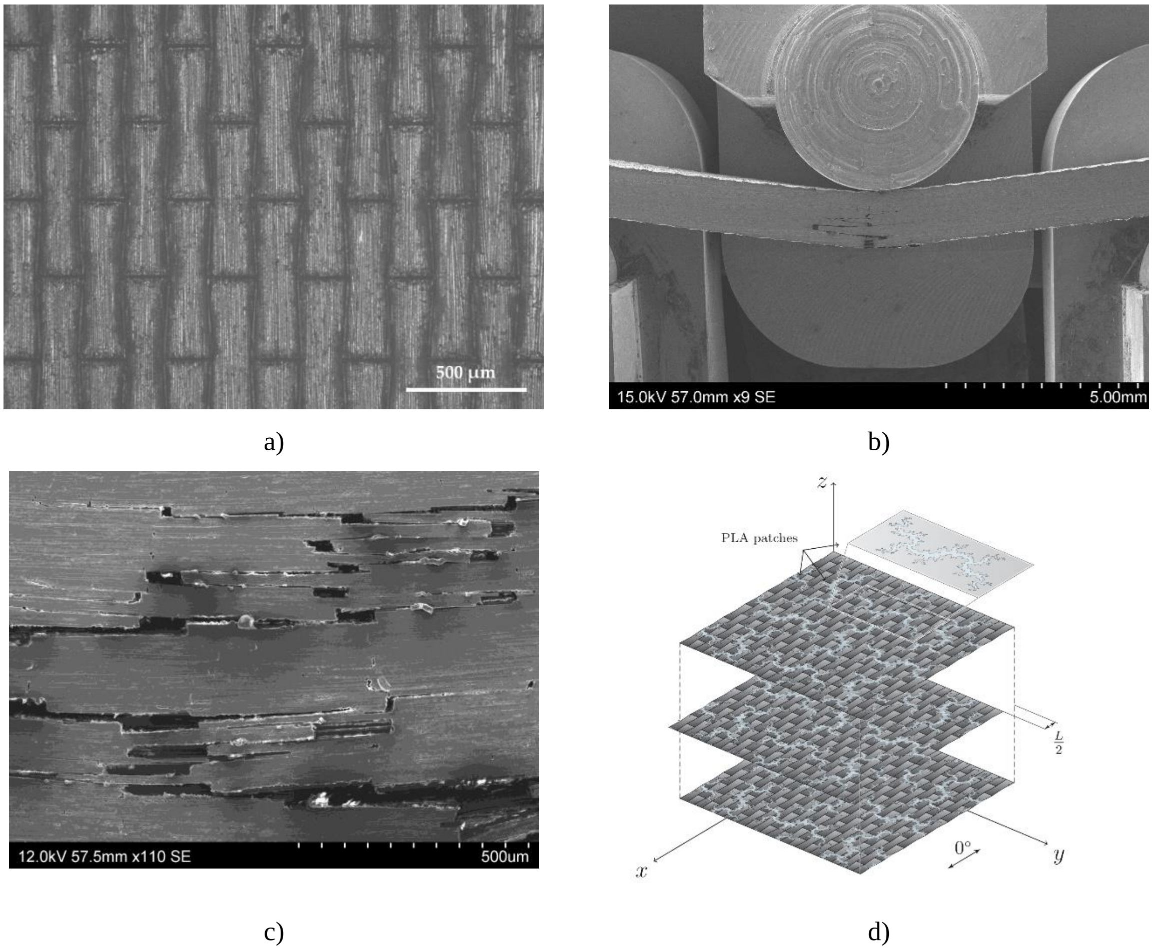


Figure 12: a) Optical micro-graph of laser-cut carbon/epoxy prepreg with interlocking micro-structure. b) SEM image showing crack deflection in the nacre-like laminate under three-point bending. c) zoom-in highlighting the crack deflection pattern and tiles pull-out. d) Schematic of nacre-inspired CFRP laminate with fractal shaped patches of PLA film at each ply interface. Reproduced and adapted from [163] with permission from *Elsevier*.

Aiming at further enhancing the damage diffusion capability of HPFR nacre-like structures, Narducci et al. [162] showed that hybridising a CFRP nacre-like microstructure with meso-layers of continuous glass fibres (Figure 13a) leads to enhancing the damage resistance of the composite. Fracture is stabilised through gradual pull-out of tiles (Figure 13b). Additionally, the meso-layers of glass fibres acted as crack arrest mechanism to the propagation of damage, further enhancing the damage resistance of the composite (Figure 13b).

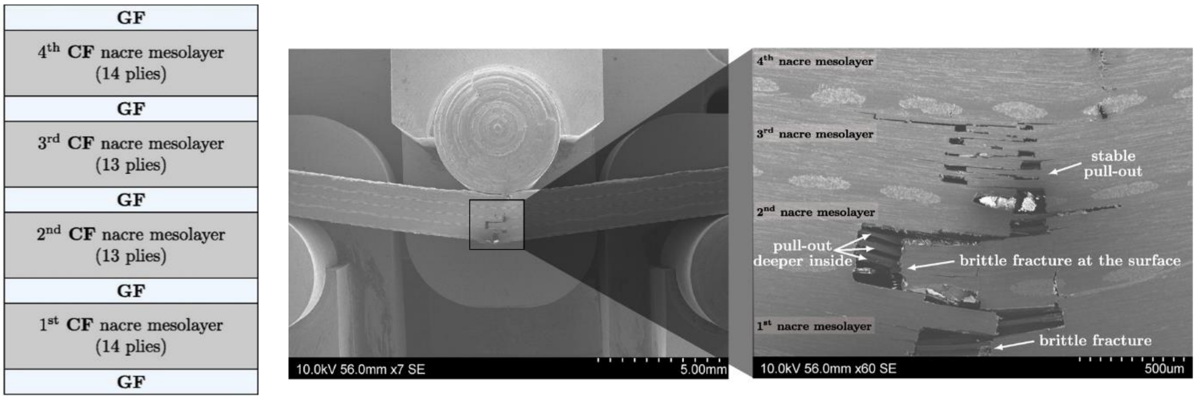


a) b)

Figure 13: a) Schematic of. layup of a hybrid Glass fibre (GF)-carbon fibre (CF) nacre composite. b) SEM image of a GF-CF nacre hybrid sample tested under three-point bending. The zoom-in of the region where failure developed highlights the presence of stable pull-out mechanism of the nacre-like microstructure as well as the activation of a crack arrest mechanism due to the presence of the glass meso-layers. Reproduced and adapted from [162] with permission from *Elsevier*.

Pascoe et al. [164] developed hybrid Titanium-CFRP nacre microstructures (Figure 14a) and tested them under three point bending and pure tension at room and high temperature. Compared to a pure CFRP nacre microstructure, the Titanium-CFRP nacre hybrid architecture showed high damage diffusion capability (Figure 14b) with the latter increasing as the interfacial bonding between titanium and CFRP decreases.

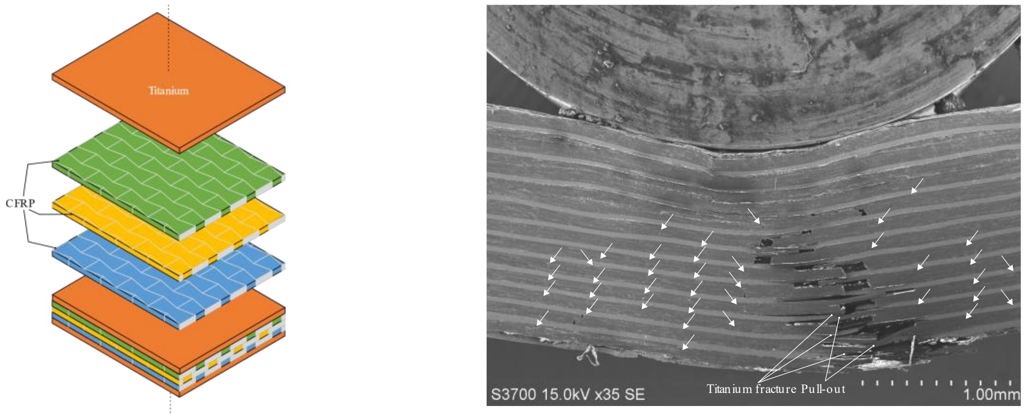


a) b)

Figure 14: a) Schematic of layup of a hybrid interleaved Titanium-CFRP nacre composite. b) SEM image of a Titanium-CFRP nacre sample tested under three-point bending highlighting how damage managed to diffuse away from the main crack path. Adapted from [164].

Overall, nacre-inspired HPFRP microstructures successfully managed to enhance volumetric energy dissipation of conventional structures by diffusing damage and promoting crack deflection. The manufacturing procedure devised to produce such microstructures makes use of conventional hand-layup and state-of-the-art laser-milling equipment to engrave the nacre pattern with micrometric precision. Despite adding an additional manufacturing step to the manufacturing of a conventional composite structures, the technique can be easily integrated into an automatic manufacturing chain, hence it lends itself to the ongoing digitalisation and automatization of the Composite Industry.

## 2.3 Bone

Table 3: Summary of recent studies dealing with the replication of tough bio-composites inspired to bone microstructures

| Ref | Manufacturing | Material | Scale | Performance enhancement & Toughening mechanisms |
|---|---|---|---|---|
| **[115]** | • PolyJet multi-materials 3D printing and in-situ curing | • Reinforcement: stiff photopolymer<br>• Matrix: soft photopolymer | • Compliant phase (soft polymer) thickness: 250 µm | • 20 times higher toughness modulus than the source material<br>• Crack deflection and stable crack propagation |
| **[71]** | • Multi-material 3D printing | • Reinforcement: stiff acrylic-based photopolymers<br>• Matrix: soft acrylic-based photopolymers | • Osteon diameter: 100-300 µm (printer resolution: 16 µm)<br>• Cement line: 4-7 µm | • Increase in toughness of one order-of-magnitude compared to bulk polymer<br>• fibril and ligament bridging, crack blunting, crack branching, crack deflection |
| **[16]** [187] | • Manual cocooning and stitching, resin injection | • Reinforcement: UD-GF and ±45° CF-NCF sleeves<br>• Matrix: epoxy<br>• Top and bottom surface: UD-GF-NCF | • Osteon diameter: 100-200 µm<br>• Sleeve diameter: 4-5 mm | • 18% lower fracture toughness and 16% lower fracture strength than the comparative composite (layered UD-GF and ±45° CF)<br>• Crack deflection, longitudinal splitting, damage diffusion |
| **[119]** | • Cold-isostatic-press compaction and sintering | • Reinforcement: Hydroxyapatite (HA)<br>• Matrix: 6-nylon | • HAp diameter: 18µm | • Comparable work of fracture with natural materials of bone (W = 137±20 J/m$^2$)<br>• Stretching of polymer ligaments, stable crack growth |
| [188] [189] [190] [191] | • Laser-engraving. Hot compaction | • Self-reinforced polypropylene (SRPP) hybridised with continuous carbon fibres. | • Laser-cut length: 1mm | • High values of fracture toughness (213 KJ/m$^2$)<br>• 90% increase in energy diffusion capability.<br>• Critical failure during impact is delayed to larger applied displacement.<br>• Damage diffusion, stable pull-outs, enhanced stretching |

### 2.3.1 Microstructure of Bone

The remarkable fracture behaviour and toughness of bone make it a promising type of structure that can serve as a model for advanced composites [2]. The major building blocks of bone's hierarchical structure are stiff hydroxyapatite platelets (HA) and flexible collagen fibres, which are concentrically aligned in lamellae, the so called in *osteons* (Figure 15) [2]. As such, the hierarchical microstructure of bone stretches over various length scales [2]. The most important toughening mechanisms for bone are crack-deflection, constrained micro-cracking, uncracked ligament-bridging and collagen-fibril bridging [54] (Figure 16). Gao et al. [31] showed that the hierarchical arrangement of staggered patterns of stiff mineral inclusions embedded in a soft matrix typical of bones allows for the activation of sliding mechanisms of the stiff inclusions along one another during deformation, resulting in a highly stable pull-out mechanism that stabilises failure and allow for large inelastic macroscopic strains. Additionally, as observed by Rabiei et al. [192], the staggered patterns of stiff inclusions lead to highly dissipative 'staircase'-type of crack paths with high energy dissipation capability.

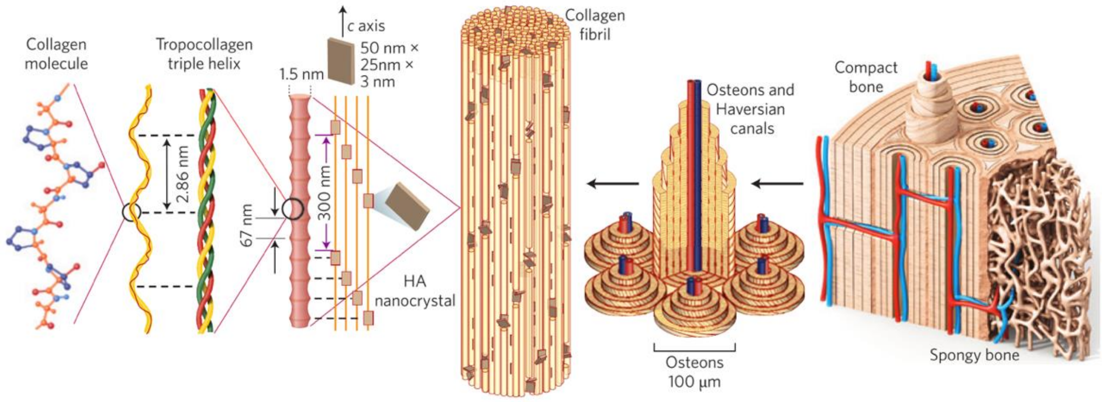


Figure 15: Schematic illustration of the hierarchical structure of cortical bone with building blocks ranging across a band of length scales. Reproduced from [17] with permission from *Springer Nature* as redrawn from [193] (©*Nature Publishing Group)* and [194] (©*The Journal of Bone and Joint Surgery)*.

### 2.3.2 Bone-inspired artificial composites

#### 2.3.2.1 Prototyped bone-inspired composites

A multi-material 3D-printing method, using both stiff and soft photopolymers, was applied by Libonati et al. [71] to mimic the *Haversian* bone system. Structures with both circular and elliptical osteons, as well as soft and stiff matrices, were investigated (Figure 16). The osteons were found to take an important role in the fracture toughness of the artificial composite due to their ability to reduce stress concentrations at the crack-tip, the formation of micro-voids which absorb energy, and the stable propagation and deviation of the cracks. Dimas et al. [115] followed the same approach based on additive manufacturing, but fabricated a composite mimicking the staggered and brick-and-mortar-like arrangement of HA and collagen in bone. Pezzotti et al. [119] developed a bone-like structure using the cold-isostatic-press-compaction (CIPC) method and a sintering process to create a well-controlled porous structure from hydroxyapatite powder (HAp).

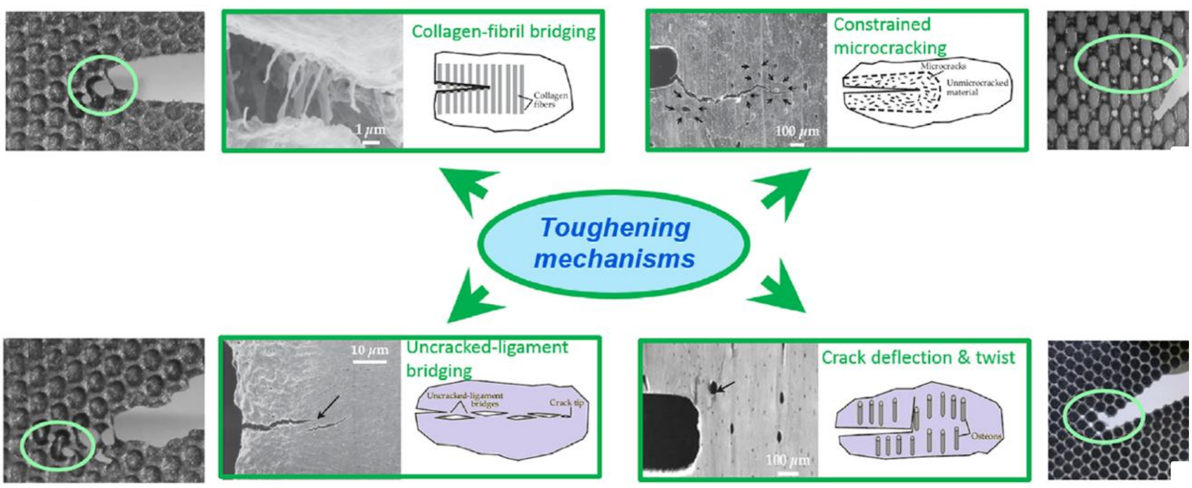

Figure 16: Toughening mechanisms observed in the bio-inspired polymer composites compared to the actual mechanisms observed in bone. Reproduced from [71] with permission from *John Wiley & Sons*, as adapted from [54] (© *American Institute of Physics*).

#### 2.3.2.2 Bone-inspired HPFRPs

Libonati et al. [16] manufactured a HPFRP laminate mimicking the *Haversian* structure, using unidirectional glass fibres (GF) as osteons, carbon fibre sleeves (CF) in ± 45° direction as 'cement-lines' around the osteons, UD-GF-non-crimp-fabric (NCF) as external layers at the top and bottom of the composite and epoxy as the matrix (Figure 17). The manufacturing process of this bio-inspired composite was complex, due to the amount of manual work that was included in cocooning the GF with CF-sleeves as well as in the stitching and cutting steps. The infiltration process was redesigned based on vacuum assisted resin injection and resin transfer moulding techniques, resulting in a fibre volume fraction of 54%. The bio-inspired composite showed the anticipated bone-like fracture mechanisms (Figure 17) such as longitudinal splitting and crack deviation, even though the fracture toughness was notably lower relative to the baseline laminate (UD-GF/CF layers enclosed by ± 45° CF-layers).

In order to improve the fracture toughness and the transverse properties of the bone-inspired composite, Libonati et al. [187] proposed multilayer osteon structures, adding both fabrics interleaved between the osteons and nano-particles with a platelet shape to the matrix. This bone-inspired microstructure was achieved with a customised technique based on hand preforming and VARTM. Tensile, compression, three-point bending, and translaminar fracture toughness tests showed that the main toughening mechanisms of bone microstructures were successfully mimicked achieving an increase in fracture toughness of up to 86% compared to previous design and to other classically designed laminated composites.

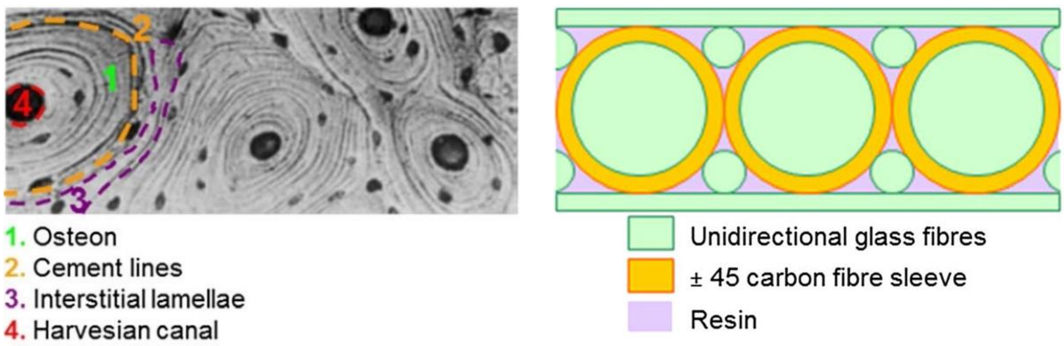


a) b)

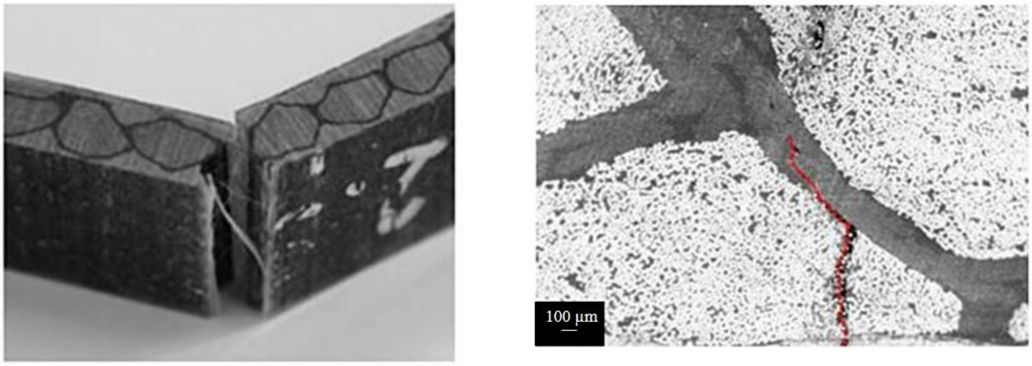


c) d)

Figure 17: a) Scanning electron microscopy (SEM) image showing the microstructure of bone and b) the schematic cross-section of the artificial bone-like composite. a) Flexural bending and fracture of bio-inspired composite and b) SEM image illustrating crack deviation from within the osteon to the inter-osteon interface. Reproduced from [16] with permission from *John Wiley and Sons*.

Bone-based hierarchical patterns of staggered discontinuities introduced across the load-carrying fibres of high-performance fibre-reinforced composites have been used to improve several aspects of the damage tolerance of self-reinforced polypropylene/carbon fibre polypropylene (SRPP/CFPP) composites [188]–[191]. Specifically, Tang et al. [188]–[190] performed extensive combined analytical/experimental analyses on the effect of hierarchical patterns on the tensile performances of a SRPP/CFPP hybrid composite consisting of single layer of CFPP sandwiched between two PP tapes. Their results showed that by using tailored hierarchical structures is possible to achieve a ‘pseudo-ductile’ tensile behaviour characterised by stable damage growth (Figure 18).

Mencattelli et al. [191] developed a multi-tailored material design framework based on the design of hierarchical patterns of discontinuities tailored to meet various damage tolerant requirements using the same technique to engineer the microstructure within the same structure. Specifically, patterns of discontinuities were tailored to: (i) increase damage diffusion (energy dissipation capability) and (ii) enhance the impact damage tolerance of a SRPP/CFPP cross ply structure. Double edge-notched tensile tests in combination with the essential work of fracture method showed that the locally-tailored regions of the structure defines high energy dissipation paths through which the structure can safely dissipate large amount of energy without leading to catastrophic failure (Figure 19a). Damage was stabilised and propagated at sub-critical levels, meaning that the structure could still operate at high loads and preserved its structural integrity. This resulted in a 90% increase in the energy dissipation capability of the structure with respect to a non-engineered baseline structure (Figure 19b) [191]. Additionally, patterns of discontinuities were successfully designed to promote damage diffusion under impact, resulting in a delay in the occurrence of penetration with respect to the non-engineered structure and increase in energy dissipated at sub-critical levels (Figure 19c) [191].

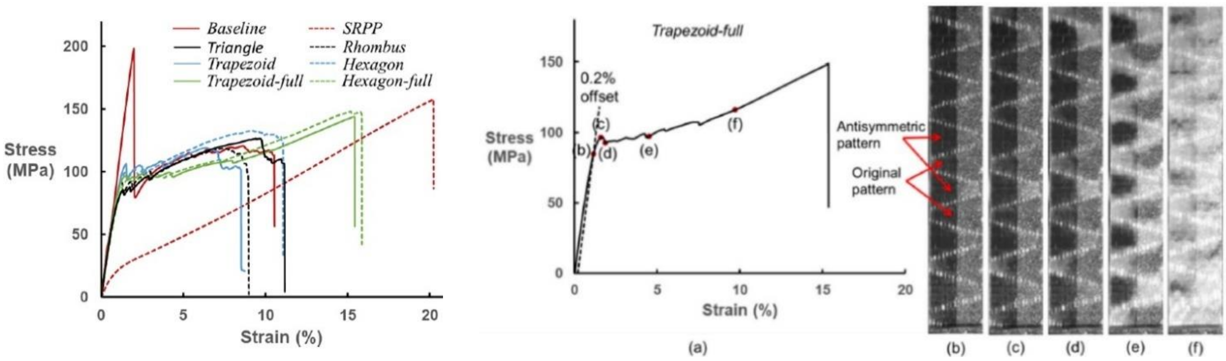


a) b)

Figure 18: a) stress strain curves of hybrid SRPP/CFPP composites with various hierarchical structures of discontinuities created with a laser-engraving technique across the carbon fibres. b) progressive damage formation under tension of a SRPP/CFPP hybrid sample with hierarchical pattern of discontinuities. Adapted from [190] with permission from *Elsevier*.

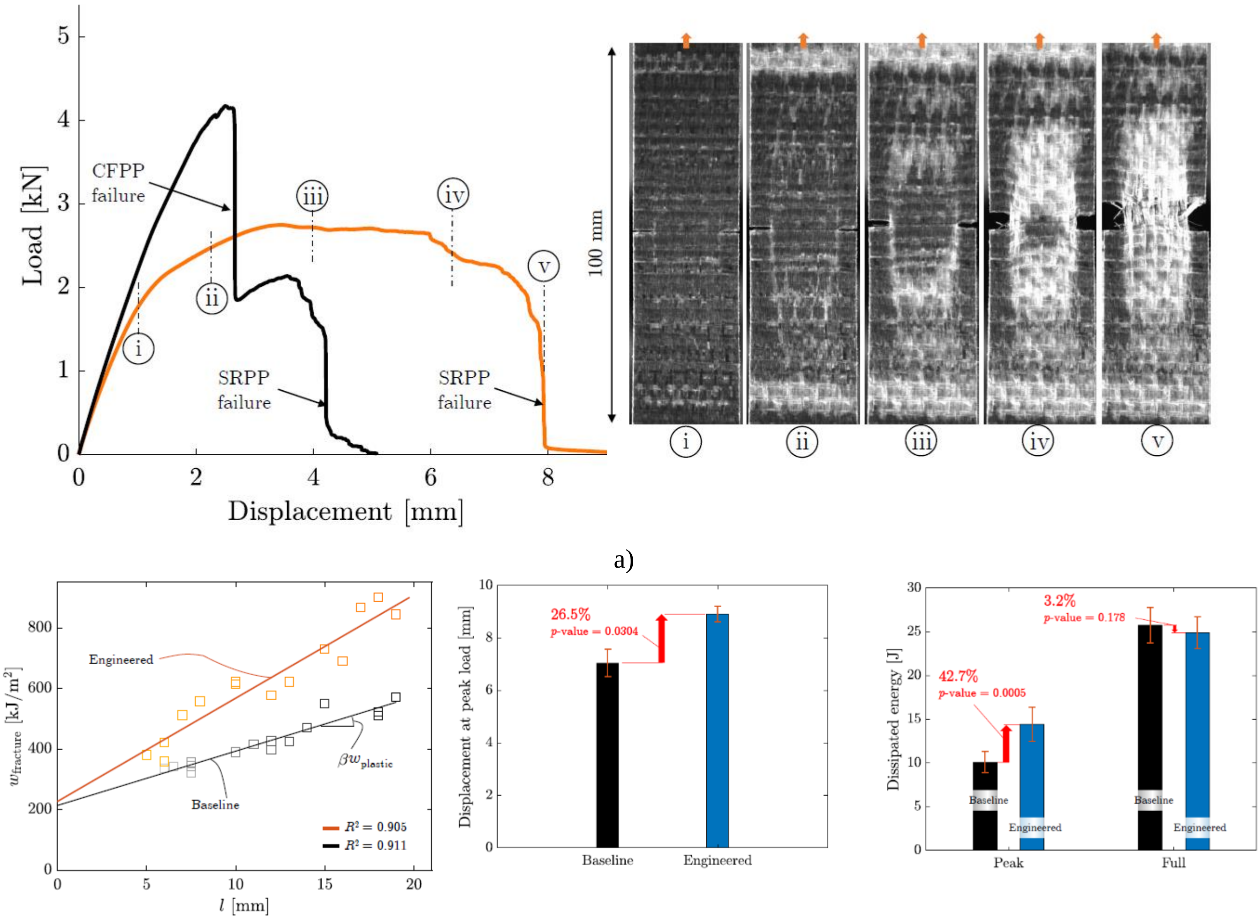


a)

b) c)

Figure 19: a) Load displacement curve of a bone-inspired SRPP/CFPP hybrid DEN-T sample highlighting the fracture process with highly diffused sub-critical damage extending away from the notch plane. b) Specific work of fracture of a SRPP/CFPP cross ply hybrid laminate with a non-engineered (baseline) and engineered plant-inspired microstructure. The tailored pattern of discontinuities resulted in a 90% increase in energy dissipation capability (slope of the specific work of fracture, $\boldsymbol{\beta w_{\text{plastic}}}$) c) Impact tests displacement at critical failure (peak-load), dissipated energy at sub-critical level (before the peak load) and total dissipated energy for a SRPP/CFPP cross ply hybrid laminate with a non-engineered (baseline) and engineered plant-inspired microstructure. Adapted from [191] with permission from *Elsevier*.

Section 2.3 has shown that several manufacturing techniques suitable to HPFRPs can be implemented to reproduce a wide range of features typical of bone microstructures. Depending on the number of hierarchical levels and complexity of features to reproduce, the related manufacturing processes can be complex (e.g. Harvesian bone-like structure devised by Libonati et al. [16], [187]). This results in prototyped structures which, due to the current limitations of the available manufacturing techniques, are not yet scalable to large structural components. The mimicking of some of the structure-functionality relationships observed in the bone microstructure rather than the exact microstructural features, allow to tailor the design to manufacturing procedures more suitable to current capabilities and engineering standards (e.g. use of laser-milling techniques). Therefore, such solutions currently offer a more suitable option to be exploited within an industrial context.

## 2.4 Plants

Table 4: Summary of recent studies dealing with the replication of tough bio-composites inspired to plant microstructures

| Ref | Manufacturing | Material | Scale | Performance enhancement & Toughening mechanisms |
|---|---|---|---|---|
| **[126]** | • Layer-by-layer (LBL) assembly in deposition process | • Reinforcement: nanofibrillated cellulose (CNF)<br>• Matrix: PVAm | • 6 layers: 35-187 nm | • Increased toughness and chain bridging with increased CNF content<br>• Fibril bridging |
| **[128]** | • 3D printing of particle and short fibre reinforced epoxy | • Reinforcement: nano-clay platelets, silicon carbide whiskers and carbon fibres<br>• Matrix: Epon 826 epoxy and DMMA | • Platelets: 1 nm x 100 nm<br>• Whiskers: 0.65 µm x 12 µm<br>• CF: 10 µm x 220 µm | • Fibre pull-outs<br>• Interface hardening |
| [195] [196] | • Laser engraved CFRP prepreg | • Reinforcement: HS-CF prepreg (TR50s)<br>• Matrix: epoxy | • 0°-ply thickness: 0.03 mm<br>• 90°-ply thickness: 0.055 mm<br>• Micro-cuts: 10-15 µm | • Stable crack growth<br>• +500% laminate work of fracture with Compact-Tension tests<br>• Large pull-out of fibre bundles<br>• Controlled debonding/sliding |

### 2.4.1 Microstructure of Plants

Plants, and particularly wood with its hierarchical structure , serve as promising models for artificial composites that are both lightweight and tough [65]. The structure of wood incorporates different cell wall layers (Figure 20). Each of these layers consists of tissue in which fibrils cross each other, form a helix or are arranged with a certain (usually steep) angle, known as Micro-Fibrillar Angle (MFA) [41], [197]. These fibres are embedded in a matrix of hemicellulose and lignin, forming the wood composite [41], [197], [198]. Along with the grade of crystallinity of the cellulose constituting the microfibrils, the MFA controls key mechanical properties of natural plant-based fibres such as Young modulus and strength [199]. Specifically, higher cellulosic content and lower MFAs, i.e. microfibril are highly aligned with the fibre axis, results in higher Young Modulus and higher tensile strength [200]–[202]. On the contrary, increasing MFAs lead to a degradation of the ultimate fibre strength and moduli with a more evident pseudo-ductile behaviour leading to larger failure strains [200]. Another factor contributing to the structural complexity is the variation in cell-wall thickness and variation in density throughout the stem [41], [197]. This typical design feature in nature is usually referred to as *graded* as shown in Figure 20.

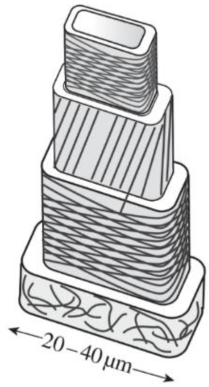


Figure 20: Multiscale cell-wall structure in wood consisting of different concentric layers showing various fibril orientations. Reproduced from [203] with permission from *The Royal Society*.

### 2.4.2 Plant-inspired artificial composites

#### 2.4.2.1 Prototyped plant-inspired composites

The hierarchical cellular structure of balsa wood and the alignment of its reinforcement were successfully mimicked by Compton and Lewis [128] using 3D-printing. With additives like nano-clay and dimethyl methyl phosphonate, they managed to print an epoxy (Epon 826) with silicon carbide whiskers ($SiC_w$) and carbon fibres. The incorporation of such reinforcements with high aspect ratio into the cellular structures (square, hexagonal, and triangular honeycomb structures) led to a substantial increase in the mechanical properties compared to the plain epoxy. Zorzetto et al. [204] developed 3D-printed wood-inspired helix-reinforced cylinders successfully demonstrating that failure resistance can be improved by using a minimum amount of fibrils in the helicoidal layer with the fibrils oriented perpendicular to the applied load.

#### 2.4.2.2 Plant-inspired HPFRPs

The use of hierarchical structures, inspired by naturally-occurring plant-based materials, has been used by Bullegas et al. [195], [196] to improve the translaminar fracture toughness of CFRP materials. Translaminar fracture consists of a through-the-thickness crack that propagates along and in-plane (ply-plane) direction under longitudinal tensile loading. When the load is aligned along the fibre direction, a translaminar crack will propagate breaking fibres. Therefore, since the strength and stiffness of a composite are greatly reduced by a translaminar crack, increasing the translaminar work of fracture can be a very effective technique to improve the damage tolerance of high-performance fibre reinforced plastics.

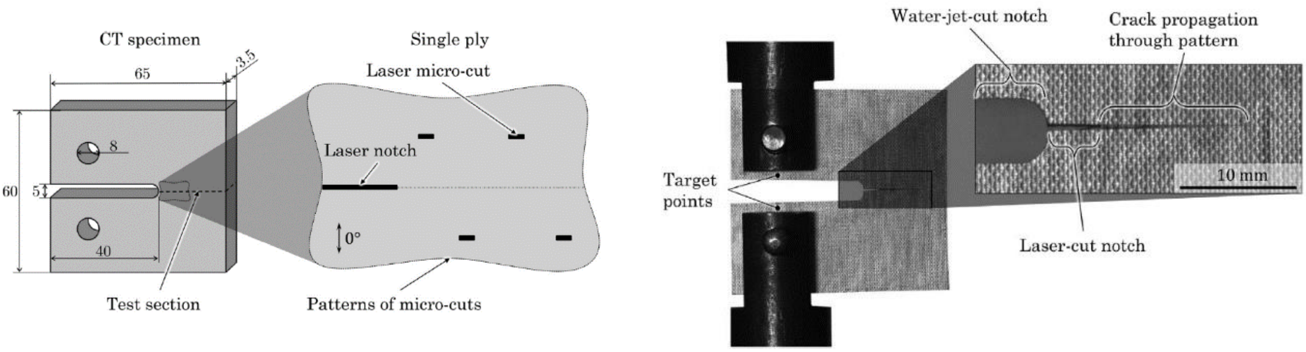


a) b)

Figure 21: a) Design of laser-engraved micro-cuts for crack deflection in CFRP and b) Compact Tension test for measurement of the translaminar fracture toughness of the pattern of micro-cuts. Reproduced from [195] with permission from *Elsevier*.

Using CFRP prepreg, Bullegas et al. [195], [196] created hierarchical micro-structures similar to those found in plants as a means to create highly-dissipative cracking patterns for improved translaminar fracture toughness. Patterns of micro-cuts perpendicular to the fibre direction (Figure 21a) were created by means of a laser-engraving technique aiming at promoting crack deflection and extensive fibre pull-out. Specifically, laser-cuts were introduced in the 0° plies of a thin-ply CFRP cross-ply composite in order to promote the formation of hierarchical pull-out of carbon fibre bundles. Compact Tension tests (Figure 21b) revealed that the presence of large pull-out structures (Figure 22) led to an increase in toughness of up to 200% for the UD lamina. Besides the formation of hierarchical pull-out structures, Bullegas et al. [196] unveiled the potential of tailored laser-cut patterns for promoting crack deflection mechanisms and failure mechanisms interaction between neighbouring plies with different fibre orientation. This design, called “shark teeth” design (Figure 22c), led to a +560% increase in work of fracture for cross-ply laminates, and about +180% for quasi-isotropic laminates (Figure 22d) with respect to baseline, non-engineered, microstructures.

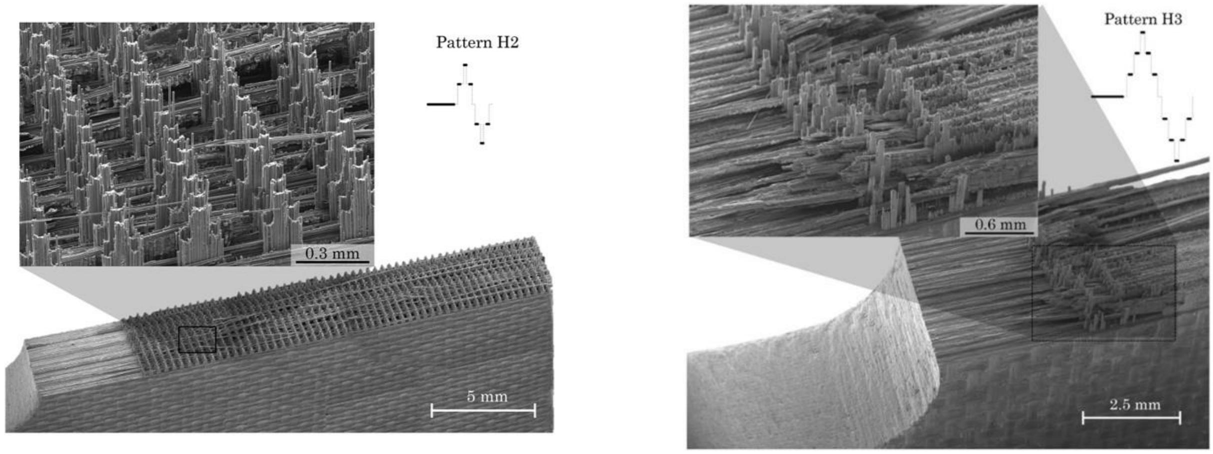


a) b)

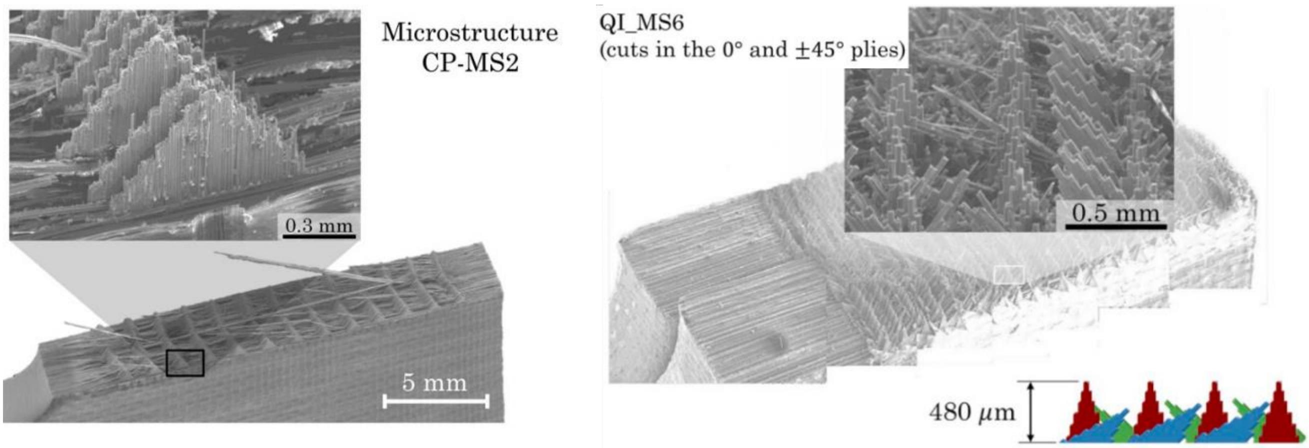


c) d)

Figure 22: SEM images of tested Compact Tension CFRP specimens with engineered fracture surface: micro-cuts with a) 2-level, b) 3-level hierarchical pattern, c) 'shark-teeth' design. d) Fracture surface of a QI sample with patterns of micro-cuts on 0° and ±45°. Adapted from [196] with permission from *Elsevier*.

Section 2.4 has shown that by mimicking the structure-functionality of plant-based microstructures with HPFRPs it is possible to greatly enhance the toughness of conventional composite structures. Similar to concepts explored with bone-like structures, the use of discontinuities in the microstructure of HPFRPs to create inhomogeneities successfully managed to activate highly dissipative failure mechanisms such as fibre-pull-out and large areal sliding. The use of micro-milling techniques based on laser equipment allows to achieve high control on the microstructural features, characterised by high reproducibility, hence suitable to be scaled up to large scale productions.

## 2.5 Crustaceans

Table 5: Summary of recent studies dealing with the replication of tough bio-composites inspired to crustaceans' microstructures

| Ref | Manufacturing | Material | Scale | Performance enhancement & Toughening mechanisms |
|---|---|---|---|---|
| [205] | • Casting, freeze-drying, hot-pressing | • Reinforcement: chitin whiskers<br>• Matrix: natural rubber and prevulcanized latex | • Whiskers: 240 nm x 15 nm | • whiskers pull-out, bridging |
| [206] | • Autoclave prepreg hand lay-up | • Reinforcement: CF-UD AS4<br>• Matrix: epoxy 3501-6 | • CF: ~7 μm (approximated value) | • Preformed holes in specimens presented an increased toughness<br>• Pull-out |
| **[70]** | • Vacuum bagged hand-layup laminate | • Reinforcement: PAN-based UD-CF (IM7)<br>• Matrix: epoxy (CYCOM 5320-1) | • CF: ~5 μm (approximated value) | • Decreases damage through the thickness compared to quasi-isotropic material<br>• Crack deflection/twisting |
| [207] | • Autoclave prepreg hand lay-up | • Carbon fibre prepreg (NCT304-1) | • ply thickness ~158 μm | • Higher energy dissipation<br>• Crack deflection/twisting, In-plane spreading of damage |
| [208] | • Autoclave prepreg hand lay-up | • Glass fibre prepreg (DA409U/S2-glass) | • ply thickness ~187 μm | • Higher interlaminar critical energy release rate that halts delamination. 83% increase in residual strength<br>• Crack deflection/twisting, In-plane spreading of damage |

| | | | | |
|---|---|---|---|---|
| [209] | • Autoclave prepreg hand lay-up | • Carbon fibre prepreg (T700/2510) | • ply thickness ~80 µm | • Higher peak load, lower displacement at critical failure, lower dissipated energy than CP<br>• Crack deflection/twisting, In-plane spreading of damage |
| [210] | • Autoclave prepreg hand lay-up | • Carbon fibre prepreg (T800/M21) | | • Higher peak load than QI with similar dissipated energy.<br>• Preserved residual (CAI) strength<br>• Crack deflection/twisting, In-plane spreading of damage |
| [211] | • Autoclave prepreg hand lay-up | • Carbon fibre prepreg (T800/M21) | • ply thickness ~125 µm | • Lower energy absorption capability and lower residual strength (CAI) than QI.<br>• Crack deflection/twisting, In-plane spreading of damage |
| [212] [213] [214] [215] [216] | • AOA prepreg hand lay-up | • Carbon-epoxy (T700/2510)<br>• Kevlar-epoxy<br>• Glass-epoxy (G10000/6510)<br>• Carbon-epoxy (T700/2510) & CF-PA6 | • ply thickness ~75 µm | • Maximum load increases with a variable pitch angle design.<br>• Optimal pitch angle depends on the material system<br>• Crack deflection/twisting, In-plane spreading of damage |
| [217] – [219] | • Autoclave prepreg hand lay-up with high-precision alignment plate | • Carbon fibre prepreg (Skyflex USN20A) | • ply thickness ~24 µm | • The smaller the pitch angle the higher the increase in damage tolerance<br>• Increase in peak load (92%), total dissipated energy (97%) and delay of critical failure (74%) with respect to QI<br>• Residual compressive strength preserved<br>• Herringbone-Bouligand higher structural integrity<br>• Disconnected delamination, damage deflection, damage diffusion |
| [220] | • Autoclave prepreg hand lay-up | • Carbon fibre prepreg (T700/2510) | • ply thickness ~80 µm | • Higher ballistic limit than QI and CP laminates<br>• Crack deflection/twisting, damage diffusion |

### 2.5.1 Microstructure of Crustaceans

A recurrent feature in the microstructure of several species of crustaceans consists of a laminated composite organized in a periodic helicoidally-stacked (Bouligand [221]) manner where each layer is made of uniaxial hard mineral fibres embedded in a soft protein-based matrix. This microstructure has been optimized by nature to withstand out-of-plane loads, such as impacts [222]. Not surprisingly, it can be frequently found in exoskeletons, acting as a protective shell from external predators, as well as in parts of the body used as chasing tools where integrity and damage-tolerance to impacts has to be guaranteed even after several strikes.

Many biological tissues containing Bouligand structures have been broadly analysed in the literature. These include crabs exoskeleton [223], [224], lobsters pincher and cuticle [223], [225]–[227] and other arthropods such as beetles [228], [229] and scarabei [230]. An example of Bouligand arrangements can be found in the dactyl clubs of the mantis shrimp, *Odontodactylus scyllarus* (Figure 23a). As reported by Patek et al. [231], these creatures are able to kill their preys by transferring high kinetic energy with accelerations up to 10,400 g and speeds of 23 $ms^{-1}$ from a stationary position. The rapid strike can generate cavitation bubbles between the cub and their prey shell. Therefore, in addition to the impact force, high stresses generating from contact act on the prey's shell [222], [231].

The high toughness and damage tolerance of the mantis shrimp is due to the microstructural organization of the periodic region, impact region and impact surface. Analysis of charge contrast secondary electron micrographs (Figure 23b) shows that cracks nucleate and nest in the volume of the periodic region between the chitin fibres, which in turn remain undamaged and can still sustain external loads [222]. Additionally, the impact region (Figure 23a) is described by several Bouligand units periodically repeated through-the-thickness of the club and characterised by a periodic out-of-plane fibre component which results in a ‘zig-zag’ type of microstructure known as Herringbone-Bouligand [232]. This complex pattern provides a means for higher compressive stiffness and stress redistribution, further improving the damage diffusion capability of classical Bouligand architectures [232].

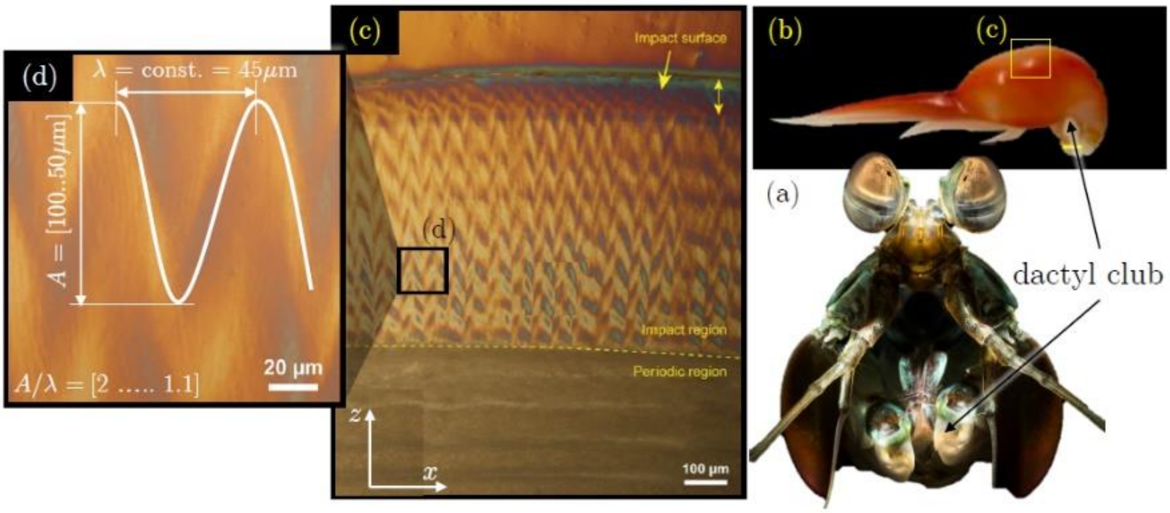


a)

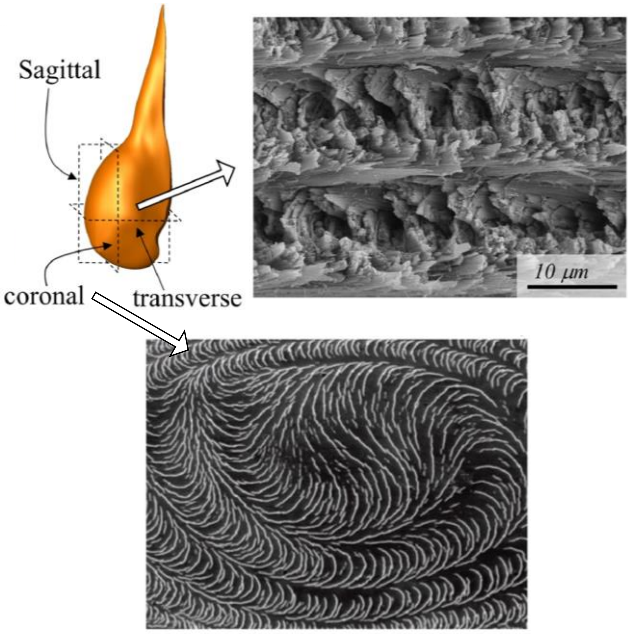


b)

Figure 23: a) Microstructure of the mantis shrimp’s dactyl club highlighting the periodic region, impact region and impact surface. A zoom-in of the impact region with a schematic of the typical Herringbone-Bouligand pattern is also reported. Reproduced from [219], [232] (© John Wiley and Sons). b) Schematic and SEM images of the coronal and transverse cross section of the dactyl club highlighting cracks nesting in the helicoidal Bouligand-like microstructure. Reproduced from [233] with permission from *Elsevier*.

### 2.5.2 Helicoidal-inspired HPFRPs

The ability of naturally-occurring helicoidal structures for diffusing damage at a sub-critical state preventing delamination and fibre failure localisation offers an outstanding opportunity to address the vulnerability of high-performance fibre-reinforced composite to through-the-thickness loads. To this end, several attempts have been made in the literature to exploit Bouligand microstructures with carbon- or glass-fibre/epoxy [70], [208], [209], [234]. Significant improvements in terms of pull-out energy [147], interlaminar fracture toughness [208], [234], residual strength [70], [208], [234] and impact resistance [70] could be observed in helicoidal bio-inspired composites, depending on the rotation (pitch) angle between adjacent plies. The resistance to crack propagation can also be attributed to the periodic variation of Young's modulus through the thickness of the composite, as described by Fratzl et al. [63] and Muarli et al. [235]. Specifically, Fratzl et al. [63] demonstrated that cracks can effectively be stopped if the ratio between the moduli of adjacent layers is larger than five (independently of the layer thickness).

Apichattrabrut and Ravi-Chandar [207] performed tensile, bending and impact tests on two Bouligand laminates (10° pitch angle), one with through-the-thickness reinforcement (z-pins) and one without z-pins. A UD specimen as well as a ±45° cross-ply laminate were tested for comparison. For both Bouligand laminates, the results showed a better debonding resistance and improved damage tolerance with respect to classical (UD and ±45° cross-ply) configurations.

Grunenfelder et al. [70], Shang et al. [209] and Liu et al. [212] investigated the impact performance of bio-inspired helicoidal carbon/epoxy prepreg-composites, in comparison with cross-ply, quasi-isotropic and unidirectional composites. Even though angles of 7.8°, 16.3° and 25.7° [70] as well as 10° and 18° [209], [212] were used for the artificial composites, which exceed the angles found in the mantis shrimp [70], small-angle-laminates have shown improved residual strength and reduced impact damage [70]. The spiralling of the crack through the thickness of the laminate (Figure 24) caused by the helical structure led to reduced fibre failure and larger delamination areas [209]. The crack front was thereby spread in-plane (Figure 24) and dissipated more energy compared to quasi-isotropic or unidirectional composites, leading to a higher toughness [70].

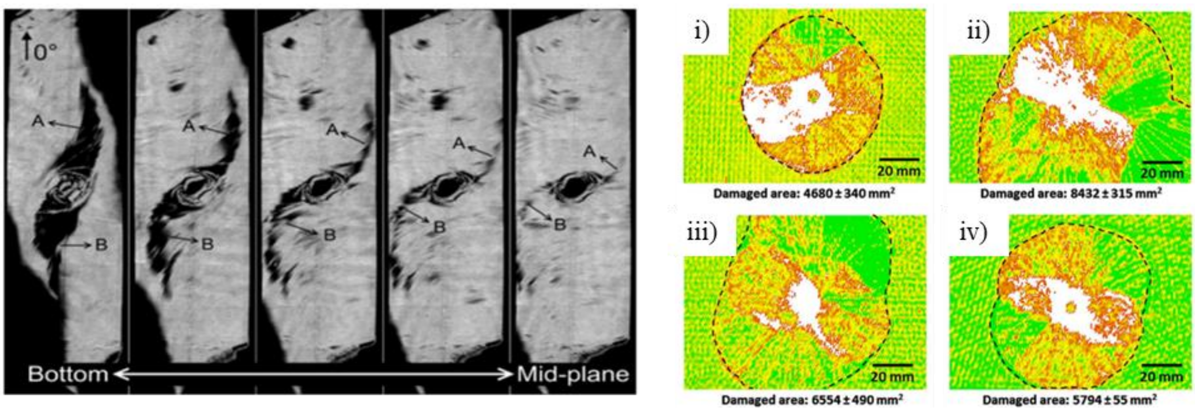

a) b)

Figure 24: a) In-plane micro-computed tomography photos of the rotating delamination front in a helicoidal carbon/epoxy composite with 10° between the adjacent plies. Reproduced from [209] with permission from *Elsevier*. b) Internal damage fields displayed in C-scans of the i) quasi-isotropic, ii) small-angle (7.8°), iii) medium-angle (16.3°) and vi) large-angle (25.7°) composite. Reproduced from [70] with permission of *Elsevier*.

Liu et al. [213], [214] tested several different CFRP Bouligand laminates (80 µm ply-thickness) showing that the maximum load-bearing capability under out-of-plane loads increases as the pitch angle decreases down to 10° (Figure 25a). However, further reducing the pitch angle leads to smaller peak load and anticipated failure with respect to a reference classical cross-ply laminate. Small pitch angles laminates (smaller than 10°) showed extensive matrix splitting which therefore lowered the performances of the laminate (Figure 25b). Laminates with optimal performances were found to present both matrix splitting, delaminations and limited fibre failure (Figure 25b).

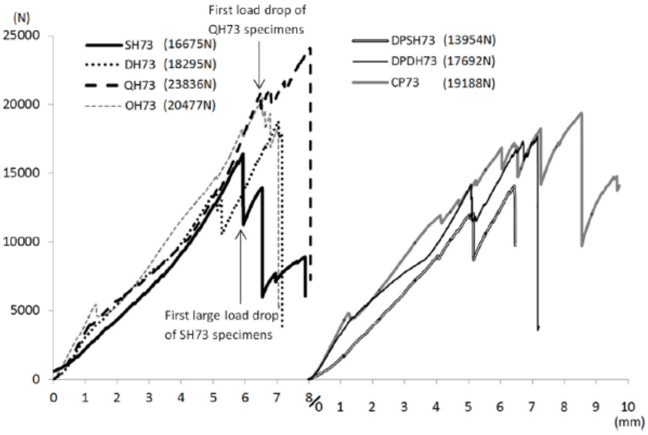


a)

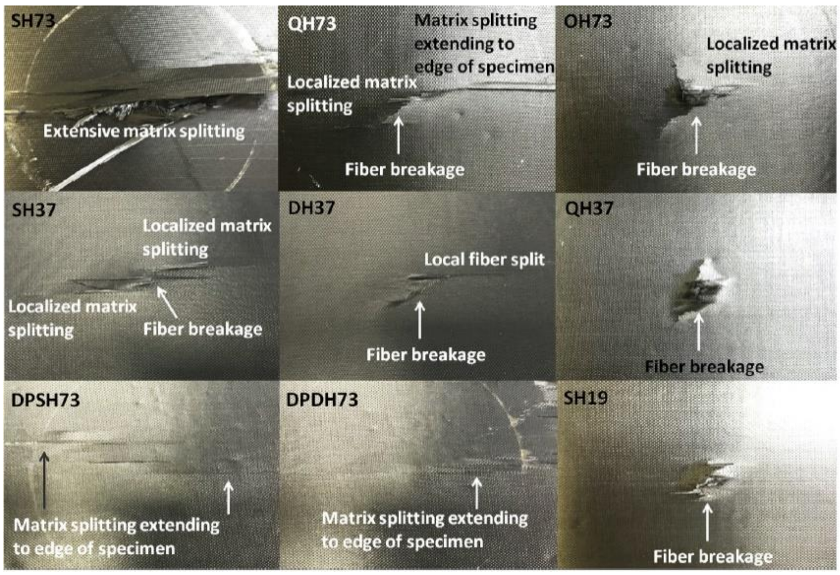


b)

Figure 25: a) Load-displacement curves of QSI tests for Bouligand-inspired laminates with different pitch angles. SH73, DH73, QH73 and OH73 are laminates with 73 plies and constant pitch angle of 2.5°, 5°, 10° and 20°, respectively. CP73 is a cross-ply laminate with 73 plies. DPSH73 and DPDH73 are laminates with 73 plies and double ply with pitch angles 5° and 10°, respectively. b) Photographs of the bottom surface of Bouligand-

inspired CFRP laminates after QSI tests highlighting the different failure mechanisms activating on the back face depending on the pitch angle Reproduced from [213] with permission of *Elsevier*.

Mencattelli and Pinho [217] developed several bio-inspired ultra-thin-ply CFRP laminates (24 µm ply-thickness) with pitch angles down to 2.5° mimicking the actual microstructure of the mantis shrimp's club. A large set of pitch angles (2.5°, 5°, 10°, 20°, 45°) was tested under low velocity impact (LVI) and compression after impact (CAI). Tests results showed that as the pitch angle decreases damage evolves helicoidally (Figure 26a-b), delamination is reduced (Figure 26c), and damage tolerance is increased via enhanced diffusion of sub-critical damage [217]. CAI tests revealed that the residual strength and failure strain did not decrease with the pitch angle, despite the steep decrease in the proportion of 0°-plies [217]. QSI-penetration and 3PB tests revealed that tailored Bouligand microstructures are capable of a simultaneous increase in load bearing capability (92%), displacement a critical failure (74%) and total dissipated energy (97%) with respect to a quasi-isotropic laminate used in engineering practice (Figure 26d) [218]. The presence of several sub-critical failure mechanisms such as twisting Bouligand matrix cracks, stable ply fragmentation and crack branching (Figure 26e) were found to be key to the outstanding enhancement in damage tolerance. A combined analytical/numerical analysis revealed that the through-the-thickness distribution of delaminations has a strong correlation with the distribution of intralaminar shear stresses in the laminate [217].

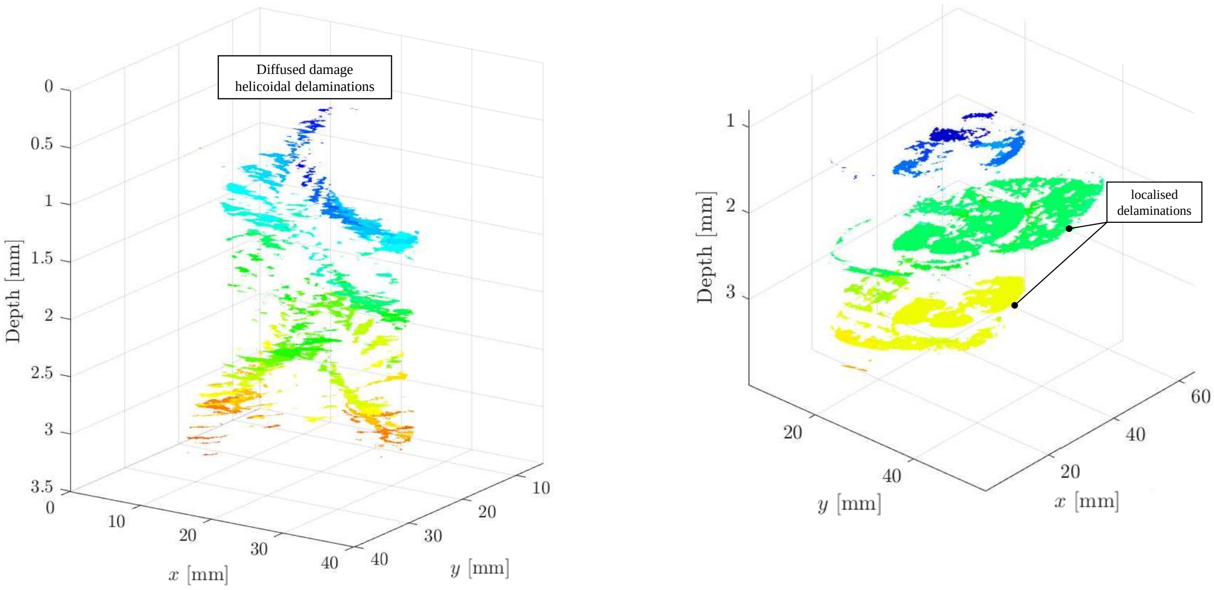


a) b)

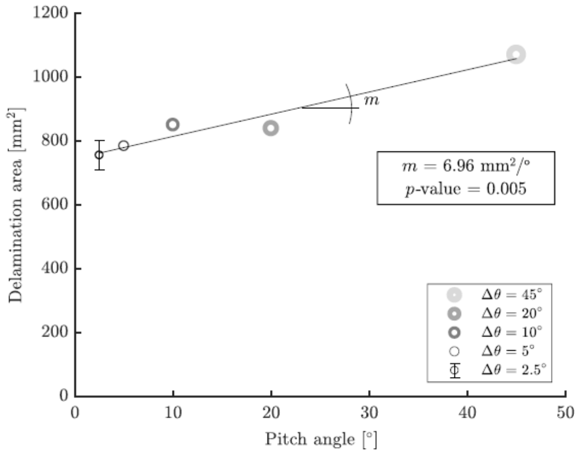


c)

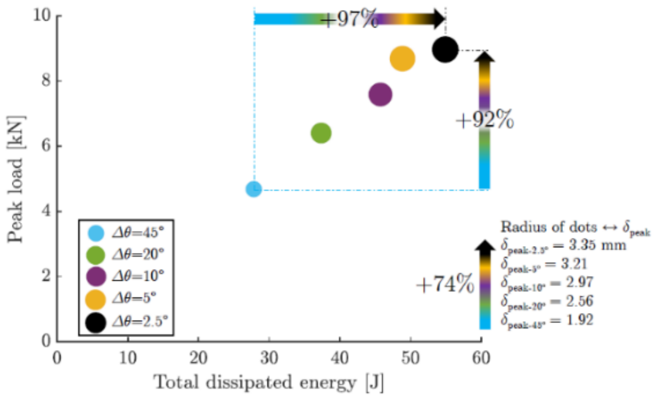


d)

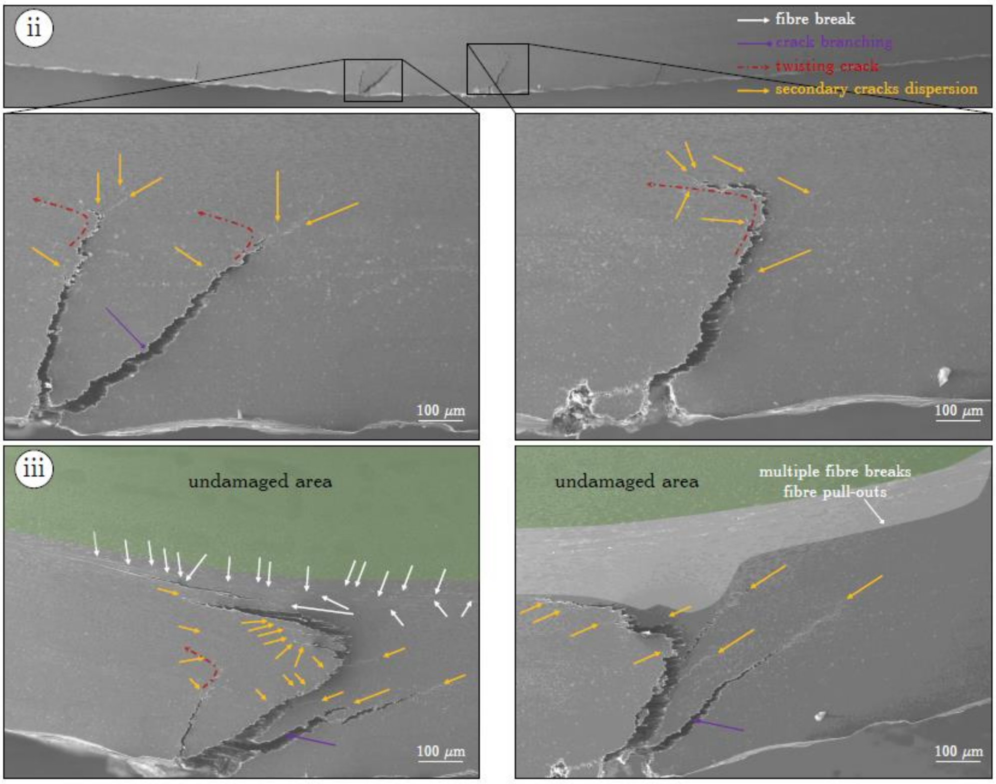


e)

Figure 26: a-b) Three-dimensional representation of the through-the-thickness distribution of delaminations (Ultrasonic C-scan) in impacted CFRP Bouligand laminates with pitch angle 2.5° and 45°, respectively. Reproduced from [217] with permission of *Elsevier*. c) Relation between pitch angle and total projected delamination area for impacted CFRP Bouligand laminates. Reproduced from [217] with permission of *Elsevier*. The results of a statistical p-value analysis are reported in [217]. d) Results of QSI tests on a wide range of Bouligand-inspired CFRP laminates highlight that reducing the pitch angle leads to a simultaneous increase in peak load, total dissipated energy and delay of catastrophic failure. Reproduced from [218] with permission of *Elsevier*. e) SEM images of a progressive 3PB tests of a 2.5° pitch angle CFRP Bouligand laminate. Reproduced from [218] with permission of *Elsevier*. Between the two load stages ii and iii, the growth of sub-critical Bouligand matrix cracks is reported in [218].

Liu et al. [214] conducted additional investigations on non-uniform distributions of pitch angle through the thickness of the laminates showing that higher peak loads can be achieved by using larger pitch angles at the back face and smaller pitch angles at the impact surface (Figure 27).

Pitch angles sufficiently large at the back surface increase the resistance to matrix splitting due to bending tensile stresses. Pitch angles sufficiently small at the impact face, where shear induced delamination normally initiates, lead to higher resistance to delamination [214].

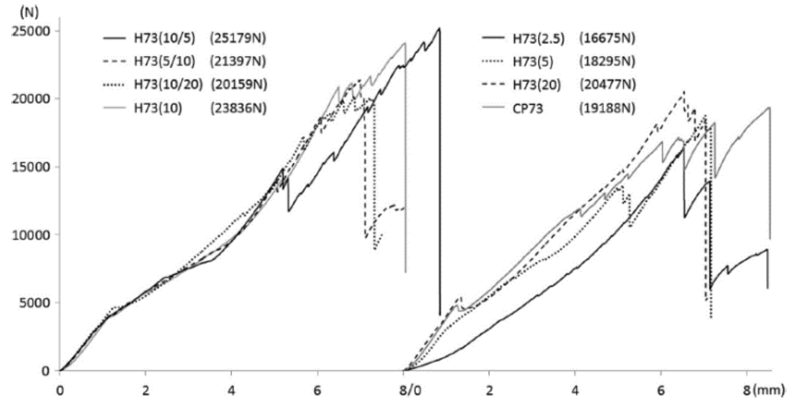


Figure 27: Load-displacement curves of QSI tests for Bouligand-inspired laminates with different pitch angles. H73(10/5) is a Bouligand laminate with 73 plies of which the bottom half with a 10° pitch angle and the upper half with 5° pitch angle. The same notation applies for H73(5/10) and H73(10/20). H73(2.5) is a Bouligand laminate with a constant pitch angle of 2.5° and 73 plies. The same notation applies to H73(5), H73(10) and H73(20) Reproduced from [214] with permission from *Elsevier*.

Several works have also explored the use of Bouligand-inspired solutions for ballistic applications [220], [236], [237]. Specifically, Liu et al [236] tested Bouligand and conventional CFRP laminates under ballistic impact showing that tailored helicoidal laminates are capable of enhanced perforation energy compared to conventional cross-ply and QI laminates (Figure 28a). Optimal Bouligand laminates with a pitch angle of 5° showed the largest increase. This was achieved via the formation of delamination damage and matrix splits acting as a stress relief mechanism to the fibres which were in turn able to stretch more, improving the impact resistance of the composite. Similar tests conducted on Kevlar®, Endumax® [236] and Dyneema® [237] fibre reinforced composites showed opposite trends (Figure 28) with the ballistic performance decreasing as the pitch angle decreases. The formation of matrix splits and helicoidal delamination damage in such helicoidal laminates lead to a mechanism which allows for the projectile to penetrate without breaking the tough fibres, thus reducing the ballistic performance of the structure.

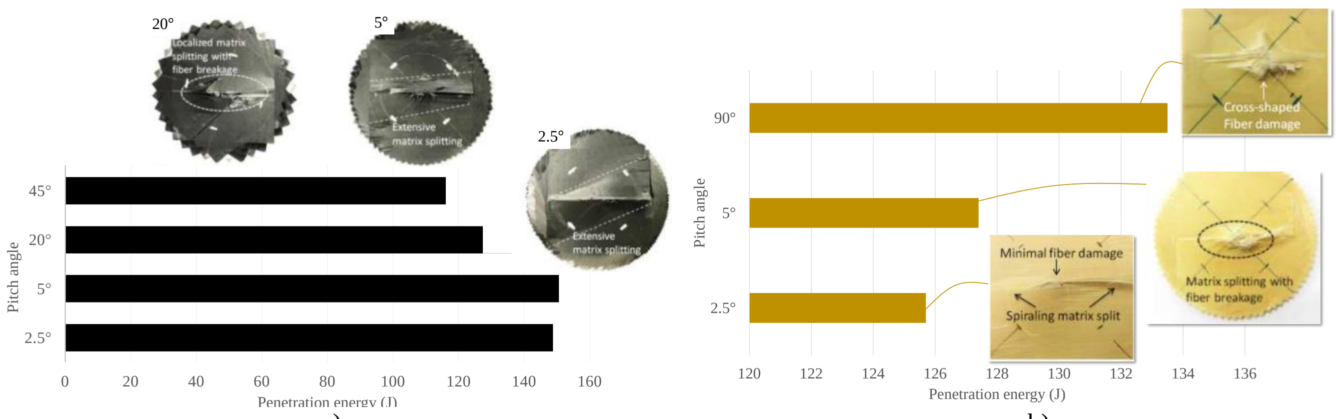

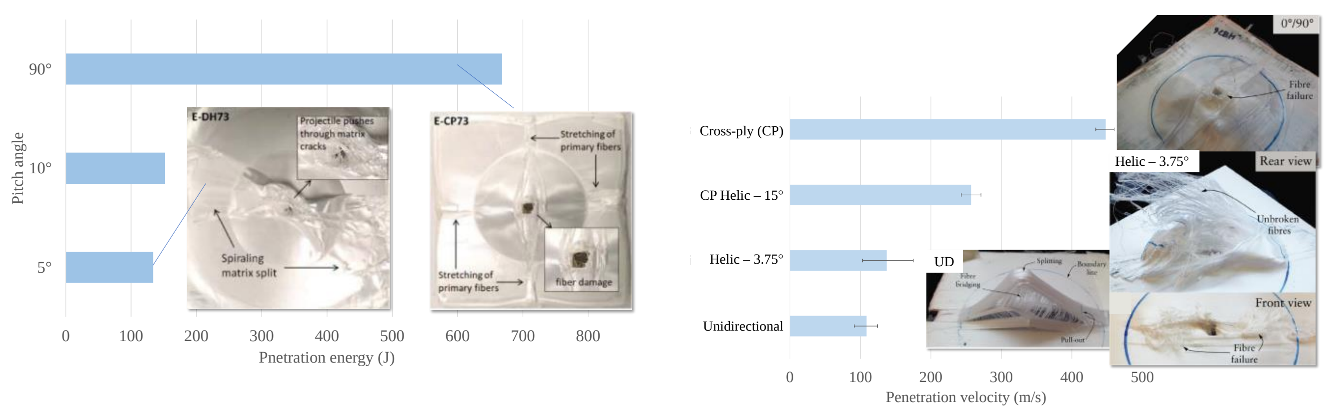


c) d)

Figure 28: Perforation energy for ballistic tests performed on helicoidal-inspired and conventional a) CFRP, b) Kevlar® and c) Endumax® laminates along with of the impacted samples. Reproduced and adapted from [236] with permission from *Elsevier*. d) Ballistic limit for Dyneema® helicoidal and conventional laminates along with photographs of impacted samples. Reproduced and adapted from [237] with permission of *Elsevier*.

The last decade of studies on Bouligand-inspired HPFRPs comprises several analytical models of twisting Bouligand cracks [217], [233], [238] and experimental investigations aiming at evaluating the effect of pitch angle [212]–[214], [217], [218], [233] fibre properties [215], matrix properties [215] and ply thickness [215] on the damage tolerance performances of the composite. All together, these studies reveal that the ability of Bouligand structures with small pitch angles for diffusing sub-critical damage in the form of helicoidal delaminations and Bouligand matrix cracks is dominated by the pitch angle, the interface/matrix properties and the ply thickness. Specifically, with increasing pitch angle, decreasing ply thickness and increasing interface/matrix toughness, the resistance to grow beneficial sub-critical helicoidal damage increases. Consequently, the probability of formation of critical failure mechanisms such as localised delamination areas and fibre failure increases [213], [215], [217], [218], thus reducing the damage tolerance to through-the-thickness loads of the composite.

The capability of tailored Bouligand structures of dissipating energy through the formation of diffused sub-critical damage was exploited by Liu et al. [216] to create CFRP solutions with intrinsic healing capability. The use of CF-PA6 Organo sheets interleaved between the layers of Bouligand CFRP-epoxy laminates led to composite solutions able to recover up to 90%, on average, of the pristine load-bearing capability under QSI [216].

In the attempt of further improving the damage tolerance of classical Bouligand structures with HPFRPs, Mencattelli and Pinho [219] designed and manufactured Herringbone-Bouligand CFRP microstructures inspired by the main features of the impact surface, impact region and periodic region of the mantis shrimp dactyl club. QSI tests comparing Herringbone-Bouligand CFRP laminates against Bouligand CFRP laminates showed that the Herringbone-Bouligand design resulted in a delay in the onset of delamination damage (Figure 29a), increased energy dissipation capability (13%), reduced in-plane spreading of damage (71%) and containment of damage within the tailored herringbone region (Figure 29b). This was achieved due to the presence of bi-sinusoidal interlocking ply-interfaces that in combination with a 2.5° pitch angle led to the formation of disconnected delamination areas, delamination deflection and accumulation of sub-critical matrix cracks on the compression side of the laminate.

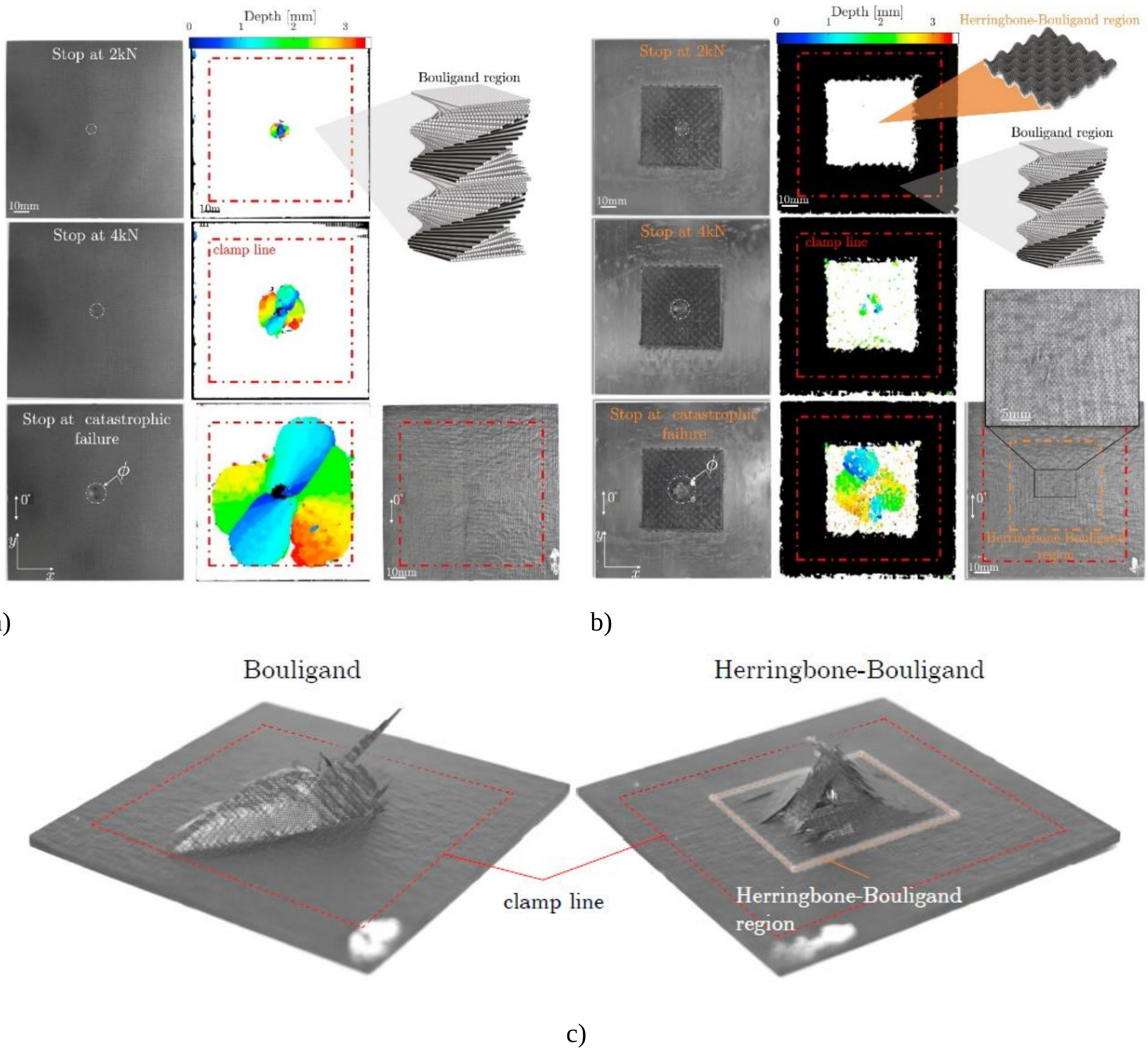


Figure 29: a) Photographs of impact face, back face and delamination damage (C-scans) of a Bouligand and Herringbone-Bouligand samples taken by interrupting the test at 2kN, 4kNand at the load drop. The figure highlights fragmented delamination area in the Herringbone-Bouligand sample with delamination mostly contained within the Herringbone region. b) Photographs of Bouligand and Herringbone-Bouligand samples at the end of QSI test (full penetration) highlighting the damage being contained inside the Herringbone region in the Herringbone-Bouligand samples while this extends up to the clamp line in the Bouligand sample. (a-c). Reproduced from [219] with permission from *Elsevier*.

With respect to HPFRP microstructures inspired by shell, bone and plants presented in this review, Bouligand-like microstructures best suit current manufacturing capabilities of the composite industry. The complexity of helicoidal composites fabrication is independent of the constituents and of the size (scale) of the component to manufacture. Helicoidal-inspired microstructures do not require the introduction of micro- or nano-scale features in the microstructure which often limits the scaling-up of bio-inspired concepts to meet industrial needs. Finally, with the continuous evolution of automated manufacturing technologies (3D printing and Automated Fibre/Tape Placement), helicoidal structures holds a tangible potential to provide composites solutions with higher structural efficiency than conventionally designed laminated structures.

# 3 Conclusions

## 3.1 Key points

Based on early endeavours to mimic biological composites, it became evident to researchers that copying nature's architectures instead of reproducing the design principles would not be a successful strategy. Biomimetics should in fact follow the basic principle of "borrowing ideas from nature for shaping and creating our surroundings" [239] without it being reduced to a blind mimic of the observed microstructures. In this context, we have shown that, by capturing the most relevant features that allow for the activation of the toughening mechanisms observed in the natural microstructures, it is possible to create HPFRP composites capable of outstanding damage tolerance, characterized by stable failure processes where several interacting sub-critical damage mechanisms dissipate energy and preserve the overall mechanical performances and structural integrity of the composite structure.

This review has summarised the latest and most relevant prototyping techniques that enable the replication of nature's toughening design principles artificially and categorized them according to their individual role-models. Certain technologies such as 3D-printing are very versatile and facilitate the fabrication of very complex structures, yet lack in the ability to realize parts down to nano-scales due to the limitations in spatial resolution. Additional prototyping techniques, such as the sintering of 3D-printed artificial composites or the multiple cutting and rearranging steps developed for the production of crossed-lamellar HPFRP have shown to hold great flexibility to create composite solutions with tailored damage tolerance.

Towards the creation of bio-inspired solutions with high technological readiness level and thus with great potential for achieving large industrial impact, manufacturing techniques such as high-precision tape placement, micro laser engraving and pre-cure microstructural moulding stem out. These powerful manufacturing tools allow engineers to deliver ready solutions in an automated manufacturing process and therefore they are suitable to be implemented in a 4.0 industrial context. The bio-inspired solutions created using these techniques, such as nacre-, plant-, bone-, Bouligand- and Herringbone-Bouligand-inspired microstructures have shown greatly enhanced damage tolerance and mechanical performance with respect to classically designed composite structures manufactured using similar techniques.

Furthermore, the review has reported the concept of bio-inspired tailorable solutions, highlighting the suitability of some bio-inspired microstructures to be tailored locally, point-by-point, in a larger composite structure. This concept was found to be a key enabler of some of the damage tolerance performance of these microstructures, such as the damage containment capability of Herringbone-Bouligand composites. Additionally, the concept provides engineers with a greatly enlarged design space for novel, more efficient composite structures tailored to custom-specific needs.

## 3.2 Applications to HPFRPs structures

In this review, we have reported on several attempts of exploiting bio-inspired designs with HPFRPs. The successful performance enhancement achieved by certain bio-inspired designs lies in the ability of these microstructures to diffuse sub-critical damage, controlling the failure process and preventing more critical and localised failure mechanisms to occur. This often results in enhanced damage resistance, structural integrity and mechanical performance of composite structures commonly used in engineering. Additionally, we have reported that many of the bio-inspired concepts, such as plant-based, bone-inspired and crustacean-inspired can be tailored point-by-point in the structure, using manufacturing techniques scalable to industrial processes and prone to be automated, hence suitable to play a major role in the Composite Industry 4.0 revolution.

The distinctive features and toughening mechanisms of the bespoke microstructures make them suitable to be tailored for different structural applications and loading conditions.

- Bone- and plant-inspired HPFRPs --- tailored patterns of discontinuities can be successfully tailored to diffuse in-plane damage achieving high increase in translaminar fracture toughness with respect to the conventional counterparts. The key aspect for the enhanced performances lies in the ability to form pull-outs and dissipate energy through friction. Therefore, such microstructural concepts would be most suitable in applications dominated by in-plane tensile loading (pure tension or bending of thin structures) and where an in-plane spreading of damage is desirable.
- Bouligand and Herringbone-Bouligand HPFRPs --- these bio-inspired solutions have shown outstanding performances under through-the-thickness loads, including quasi-static loads, low velocity and ballistic impacts. Additionally, depending on the ply thickness it has been shown that Bouligand configurations tend to spread damage in-plane (thick plies) rather than through-the-thickness (thin-ply). Therefore, depending on the specific application Bouligand solutions can be designed in combination with the choice of ply thickness to promote in-plane or through-the-thickness damage diffusion. Two major mechanisms govern the formation of sub-critical damage in helicoidal-inspired laminates: helicoidal delamination damage (shear-driven) and twisting Bouligand cracks (bending driven). Therefore, applications governed by through-the-thickness shear loads will benefit more by the formation of helicoidal delaminations while applications with a predominant bending loading will benefit more from the formation of twisting Bouligand cracks. Furthermore, since Bouligand and Herringbone-Bouligand solutions are characterised by a continuous fibre type of microstructure, they lend themselves to be used in high load-bearing applications.
- Nacre-inspired and Giga shell-inspired HPFRPs – these bio-inspired solutions are capable of achieving failure mechanisms typical of biological materials difficult to mimic with HPFRPs (e.g. crack deflection, crack branching). This results in a highly stable, highly dissipative failure with high potential to be exploited in crushing and energy absorption structures (e.g. an-intrusion shields).

### 3.3 Future Challenges

In order to exploit the full potential of nature's toughening mechanisms in bio-inspired HPFRP composites, new manufacturing techniques and processes will need to be developed, which allow for the replication of more hierarchical levels over a greater length scale. This will ultimately aid the implementation of the large series of toughening mechanisms typically found in nature.

In this context, additive manufacturing, automatic fibre placement and micro-moulding and texturing techniques will be key due to the constantly increasing range of materials that can be used with such techniques and the ever-increasing quality and complexity of the features that can be tailored point-by-point locally in the structure.

A deeper understanding of the interaction and balance between the constituents as well as the multifunctionality of the complex biological microstructures will be paramount to design future generation of bio-inspired synthetic composite materials.

Additionally, the bio-inspired HFRPs presented in this work have been often designed and tested under specific testing and loading conditions, aiming at exploiting specific toughening mechanisms. Several mechanical properties under different loading conditions remain unexplored and ought to be investigated to fully prove that bio-inspired designs can offer a robust alternative to current composite solutions. Finally, beside proofing a benefit in the use of bio-inspired HPFRP composites over conventional solutions in terms of mechanical and damage tolerance performances, the focus should be directed towards establishing a benefit in terms of weight saving (while preserving the performances of current composite structures). This is a key enabler of the use of the presented bio-inspired HPFRP designs in large scale industrial applications.

## ACKNOWLEDGMENT

F. Narducci and S.T. Pinho would like to acknowledge funding from EPSRC under grant EP/M002500/1. L. Mencattelli acknowledges the European Union’s Horizon 2020 for the funding received within the Marie Skłodowska-Curie grant agreement No 722626 (see www.fibremodproject.eu).

## REFERENCES

[1] Z. Xia, “Part I: Biomimetic Structural Materials and Processing - Strong, Tough, and Lightweigh Materials,” in *Biomimetic Principles and Design of Advanced Engineering Materials*, 1st ed., Chichester (UK): John Wiley & Sons, Ltd, 2016, pp. 13–48.

[2] F. Libonati, “Bio-inspired composites: Using nature to tackle composite limitations,” in *Advanced Engineering Materials and Modeling*, 2016, pp. 165–190.

[3] R. O. Ritchie, “Armoured oyster shells,” *Nat. Mater.*, vol. 13, no. 5, pp. 435–437, 2014, doi: 10.1038/nmat3956.

[4] W. Yang, I. H. Chen, B. Gludovatz, E. A. Zimmermann, R. O. Ritchie, and M. A. Meyers, “Natural flexible dermal armor,” *Advanced Materials*, vol. 25, no. 1. pp. 31–48, 2013, doi: 10.1002/adma.201202713.

[5] P. Vukusic and J. R. Sambles, “Photonic structures in biology,” *Nature*, vol. 424, no. 6950. pp. 852–855, 2003, doi: 10.1038/nature01941.

[6] B. Bhushan, “Biomimetics: Lessons from Nature - an overview,” *Philos. Trans. R. Soc. A Math. Phys. Eng. Sci.*, vol. 367, no. 1893, pp. 1445–1486, 2009, doi: 10.1098/rsta.2009.0011.

[7] M. A. Meyers, P.-Y. Chen, A. Y.-M. Lin, and Y. Seki, “Biological materials: Structure and mechanical

properties," *Prog. Mater. Sci.*, vol. 53, pp. 1–206, 2008, doi: 10.1016/j.pmatsci.2007.05.002.

[8] Q. Cheng, L. Jiang, and Z. Tang, "Bioinspired layered materials with superior mechanical performance via interface design," in *Technical Proceedings of the 2014 NSTI Nanotechnology Conference and Expo, NSTI-Nanotech 2014*, 2014, vol. 2, pp. 235–238.

[9] A. R. Studart, "Towards high-performance bioinspired composites," *Adv. Mater.*, vol. 24, no. 37, pp. 5024–5044, 2012, doi: 10.1002/adma.201201471.

[10] C. Zhang, D. A. Mcadams, and J. C. Grunlan, "Nano/Micro-Manufacturing of Bioinspired Materials: a Review of Methods to Mimic Natural Structures," *Advanced materials (Deerfield Beach, Fla.)*, vol. 28, no. 30. pp. 6292–6321, 2016, doi: 10.1002/adma.201505555.

[11] C. Viney and F. I. Bell, "Inspiration versus duplication with biomolecular fibrous materials: Learning nature's lessons without copying nature's limitations," *Curr. Opin. Solid State Mater. Sci.*, vol. 8, pp. 165–171, 2004, doi: 10.1016/j.cossms.2004.03.001.

[12] U. G. K. Wegst and M. F. Ashby, "The mechanical efficiency of natural materials," *Philos. Mag.*, pp. 2167–2181, doi: 10.1080/14786430410001680935.

[13] A. Ghazlan, T. D. Ngo, and P. Tran, "Three-dimensional Voronoi model of a nacre-mimetic composite structure under impulsive loading," *Compos. Struct.*, vol. 153, pp. 278–296, 2016, doi: 10.1016/j.compstruct.2016.06.020.

[14] E. Munch, M. E. Launey, D. H. Alsem, E. Saiz, A. P. Tomsia, and R. O. Ritchie, "Tough, bio-inspired hybrid materials," *Science (80-. ).*, vol. 322, no. 5907, pp. 1516–1520, 2008, doi: 10.1126/science.1164865.

[15] H. D. Espinosa, A. L. Juster, F. J. Latourte, O. Y. Loh, D. Gregoire, and P. D. Zavattieri, "Tablet-level origin of toughening in abalone shells and translation to synthetic composite materials.," *Nat. Commun.*, vol. 2, no. 173, pp. 1–9, 2011, doi: 10.1038/ncomms1172.

[16] F. Libonati, C. Colombo, and L. Vergani, "Design and characterization of a biomimetic composite inspired to human bone," *Fatigue Fract. Eng. Mater. Struct.*, vol. 37, pp. 772–781, 2014, doi: 10.1111/ffe.12172.

[17] U. G. K. Wegst, H. Bai, E. Saiz, A. P. Tomsia, and R. O. Ritchie, "Bioinspired structural materials," *Nat. Mater.*, vol. 14, no. 1, pp. 23–36, 2015, doi: 10.1038/nmat4089.

[18] S. E. Naleway, M. M. Porter, J. McKittrick, and M. A. Meyers, "Structural Design Elements in Biological Materials: Application to Bioinspiration," *Advanced Materials*, vol. 27, no. 37. pp. 5455–5476, 2015, doi: 10.1002/adma.201502403.

[19] F. Barthelat, "Designing nacre-like materials for simultaneous stiffness, strength and toughness: Optimum materials, composition, microstructure and size," *J. Mech. Phys. Solids*, vol. 73, pp. 22–37, 2014, doi: 10.1016/j.jmps.2014.08.008.

[20] L. T. Kuhn-Spearing, H. Kessler, E. Chateau, R. Ballarini, A. H. Heuer, and S. M. Spearing, "Fracture mechanisms of the Strombus gigas conch shell: implications for the design of brittle laminates," *J. Mater. Sci.*, vol. 31, pp. 6583–6594, 1996, doi: 10.1007/BF00356266.

[21] J. Sun and B. Bhushan, "Hierarchical structure and mechanical properties of nacre: A review," *RSC Advances*, vol. 2, no. 20. pp. 7617–7632, 2012, doi: 10.1039/c2ra20218b.

[22] G. Karambelas, S. Santhanam, and Z. N. Wing, "Strombus gigas inspired biomimetic ceramic composites via SHELL - Sequential Hierarchical Engineered Layer Lamination," *Ceram. Int.*, vol. 39, no. 2, pp. 1315–1325, 2013, doi: 10.1016/j.ceramint.2012.07.067.

[23] B. Pokroy, S. H. Kang, L. Mahadevan, and J. Aizenberg, "Self-Organization of a Mesoscale Bristle into Ordered, Hierarchical Helical Assemblies," *Science (80-. ).*, vol. 323, pp. 237–240, 2009, doi: 10.1126/science.1165607.

[24] R. Weinkamer and P. Fratzl, "Mechanical adaptation of biological materials - The examples of bone and wood," in *Materials Science and Engineering C*, 2011, vol. 31, no. 6, pp. 1164–1173, doi: 10.1016/j.msec.2010.12.002.

[25] K. Brandt, M. F. H. Wolff, V. Salikov, S. Heinrich, and G. A. Schneider, "A novel method for a multi-level hierarchical composite with brick-and-mortar structure," *Sci. Rep.*, vol. 2322, pp. 1–8, 2013, doi:

10.1038/srep02322.

[26] F. Barthelat, “Architectured materials in engineering and biology: Fabrication, structure, mechanics and performance,” *Int. Mater. Rev.*, vol. 60, no. 8, pp. 413–430, 2015, doi: 10.1179/1743280415Y.0000000008.

[27] H. D. Espinosa, T. Filleter, and M. Naraghi, “Multiscale experimental mechanics of hierarchical carbon-based materials,” *Adv. Mater.*, vol. 24, no. 21, pp. 2805–2823, 2012, doi: 10.1002/adma.201104850.

[28] P.-Y. Y. Chen, J. McKittrick, and M. A. Meyers, “Biological materials: Functional adaptations and bioinspired designs,” *Prog. Mater. Sci.*, vol. 57, no. 8, pp. 1492–1704, Nov. 2012, doi: 10.1016/J.PMATSCI.2012.03.001.

[29] M. J. Buehler, “Multiscale mechanics of biological and biologically inspired materials and structures,” *Acta Mech. Solida Sin.*, vol. 23, no. 6, pp. 471–483, 2010, doi: 10.1016/S0894-9166(11)60001-3.

[30] A. P. Garcia, D. Sen, and M. J. Buehler, “Hierarchical silica nanostructures inspired by diatom algae yield superior deformability, toughness, and strength,” *Metall. Mater. Trans. A Phys. Metall. Mater. Sci.*, vol. 42, no. 13, pp. 3889–3897, 2011, doi: 10.1007/s11661-010-0477-y.

[31] H. Gao, “Application of fracture mechanics concepts to hierarchical biomechanics of bone and bone-like materials,” in *International Journal of Fracture*, 2006, vol. 138, no. 1–4, pp. 101–137, doi: 10.1007/s10704-006-7156-4.

[32] K. S. Katti and D. R. Katti, “Why is nacre so tough and strong?,” *Mater. Sci. Eng. C*, vol. 26, no. 8, pp. 1317–1324, 2006, doi: 10.1016/j.msec.2005.08.013.

[33] A. Dutta and S. A. Tekalur, “Synthetic staggered architecture composites,” *Mater. Des.*, vol. 46, pp. 802–808, 2013, doi: 10.1016/j.matdes.2012.11.018.

[34] I. Su and M. J. Buehler, “Nanomechanics of silk: the fundamentals of a strong, tough and versatile material,” *Nanotechnology*, vol. 27, pp. 1–15, 2016, doi: 10.1088/0957-4484/27/30/302001.

[35] F. Barthelat and R. Rabiei, “Toughness amplification in natural composites,” *J. Mech. Phys. Solids*, vol. 59, no. 4, pp. 829–840, 2011, doi: 10.1016/j.jmps.2011.01.001.

[36] S. Haldar, N. Gheewala, K. J. Grande-Allen, M. A. Sutton, and H. A. Bruck, “Multi-scale Mechanical Characterization of Palmetto Wood using Digital Image Correlation to Develop a Template for Biologically-Inspired Polymer Composites,” *Exp. Mech.*, vol. 51, no. 4, pp. 575–589, 2011, doi: 10.1007/s11340-010-9422-7.

[37] B. Ji and H. Gao, “Mechanical Principles of Biological Nanocomposites,” *Annu. Rev. Mater. Res.*, vol. 40, no. 1, pp. 77–100, 2010, doi: 10.1146/annurev-matsci-070909-104424.

[38] J. Aizenberg, J. C. Weaver, M. S. Thanawala, V. C. Sundar, D. E. Morse, and P. Fratzl, “Skeleton of Euplectella sp .: Structural Hierarchy from the Nanoscale to the Macroscale,” *Science (80-. ).*, vol. 309, pp. 275–278, 2005, doi: 10.1126/science.1112255.

[39] J. W. C. Dunlop and P. Fratzl, *Biological Composites*. 2010.

[40] F. Bosia, T. Abdalrahman, and N. M. Pugno, “Investigating the role of hierarchy on the strength of composite materials: Evidence of a crucial synergy between hierarchy and material mixing,” *Nanoscale*, vol. 4, no. 4, pp. 1200–1207, 2012, doi: 10.1039/c2nr11664b.

[41] P. Fratzl and R. Weinkamer, “Nature’s hierarchical materials,” *Progress in Materials Science*, vol. 52, no. 8. Elsevier Ltd, pp. 1263–1334, 2007, doi: 10.1016/j.pmatsci.2007.06.001.

[42] G. L. . Bonderer L.J, Studart A.R, “Bioinspired Design and Assembly of Platelet Reinforced Polymer Films,” *Science (80-. ).*, vol. 319, pp. 1069–1073, 2008, doi: 10.1126/science.1148726.

[43] D. Sen and M. J. Buehler, “Structural hierarchies define toughness and defect-tolerance despite simple and mechanically inferior brittle building blocks,” *Sci. Rep.*, vol. 1, no. 35, pp. 1–9, 2011, doi: 10.1038/srep00035.

[44] L. Nicolais, A. Borzacchiello, M. A. Autiello, L. Russo, and L. Nicolais, “Novel Biomimetic Design for Composite Material,” in *Wiley Encyclopedia of Composites*, 2nd ed., L. Nicolais and A. Borzacchiello, Eds. John Wiley & Sons, Inc, 2012, pp. 1–8.

[45] M. E. Launey, E. Munch, D. H. Alsem, E. Saiz, A. P. Tomsia, and R. O. Ritchie, “A novel biomimetic

approach to the design of high-performance ceramic - Metal composites," *J. R. Soc. Interface*, vol. 7, no. 46, pp. 741–753, 2010, doi: 10.1098/rsif.2009.0331.

[46] T. Keplinger, E. Cabane, J. K. Berg, J. S. Segmehl, P. Bock, and I. Burgert, "Smart Hierarchical Bio-Based Materials by Formation of Stimuli-Responsive Hydrogels inside the Microporous Structure of Wood," *Adv. Mater. Interfaces*, vol. 3, no. 16, pp. 1–6, 2016, doi: 10.1002/admi.201600233.

[47] A. S. Schenk *et al.*, "Hierarchical calcite crystals with occlusions of a simple polyelectrolyte mimic complex biomineral structures," *Adv. Funct. Mater.*, vol. 22, no. 22, pp. 4668–4676, 2012, doi: 10.1002/adfm.201201158.

[48] S. Kamat, H. Kessler, R. Ballarini, M. Nassirou, and A. H. Heuer, "Fracture mechanisms of the Strombus gigas conch shell: II-micromechanics analyses of multiple cracking and large-scale crack bridging," *Acta Mater.*, vol. 52, no. 8, pp. 2395–2406, 2004, doi: 10.1016/j.actamat.2004.01.030.

[49] K. Chen, X. Tang, Y. Yue, H. Zhao, and L. Guo, "Strong and Tough Layered Nanocomposites with Buried Interfaces," *ACS Nano*, vol. 10, pp. 4816–4827, 2016, doi: 10.1021/acsnano.6b01752.

[50] F. Barthelat, "Biomimetics for next generation materials.," *Philos. Trans. A. Math. Phys. Eng. Sci.*, vol. 365, pp. 2907–2919, 2007, doi: 10.1098/rsta.2007.0006.

[51] M. J. Buehler, "Multiscale aspects of mechanical properties of biological materials," *J. Mech. Behav. Biomed. Mater.*, vol. 4, no. 2, pp. 125–127, 2011, doi: 10.1016/j.jmbbm.2010.12.018.

[52] Q. Chen and N. M. Pugno, "Bio-mimetic mechanisms of natural hierarchical materials : A review," *J. Mech. Behav. Biomed. Mater.*, vol. 19, pp. 3–33, 2013, doi: 10.1016/j.jmbbm.2012.10.012.

[53] A. Act *et al.*, "Hierarchical fibre composite structure and micromechanical properties of phosphatic and calcitic brachiopod shell biomaterials — an overview," *Mineral. Mag.*, vol. 72, no. 2, pp. 541–562, 2008, doi: 10.1180/minmag.2008.072.2.541.

[54] R. O. Ritchie, M. J. Buehler, and P. Hansma, "Plasticity and toughness in bone," *Phys. Today*, vol. 62, no. 6, pp. 41–47, 2009, doi: 10.1063/1.3156332.

[55] P. Y. Chen *et al.*, "Structure and mechanical properties of selected biological materials," *J. Mech. Behav. Biomed. Mater.*, vol. 1, no. 3, pp. 208–226, 2008, doi: 10.1016/j.jmbbm.2008.02.003.

[56] M. E. Launey, M. J. Buehler, and R. O. Ritchie, "On the Mechanistic Origins of Toughness in Bone," *Annu. Rev. Mater. Res.*, vol. 40, no. 1, pp. 25–53, 2010, doi: 10.1146/annurev-matsci-070909-104427.

[57] P. Benjwal and K. Balani, "Multi-Length Scale Hierarchy in Natural Materials," in *Biosurfaces: A Materials Science and Engineering Perspective*, 2015, pp. 146–169.

[58] R. O. Ritchie, "Mechanisms of fatigue-crack propagation in ductile and brittle solids," in *International Journal of Fracture*, 1999, vol. 100, no. 1, pp. 55–83, doi: 10.1023/A:1018655917051.

[59] N. K. Simha, F. D. Fischer, O. Kolednik, J. Predan, and G. X. Shan, "Crack tip shielding or anti-shielding due to smooth and discontinuous material inhomogeneities," *Int. J. Fract.*, vol. 135, no. 1–4, pp. 73–93, 2005, doi: 10.1007/s10704-005-3944-5.

[60] N. K. Simha, F. D. Fischer, O. Kolednik, and C. R. Chen, "Inhomogeneity effects on the crack driving force in elastic and elastic-plastic materials," *J. Mech. Phys. Solids*, vol. 51, no. 1, pp. 209–240, 2003, doi: 10.1016/S0022-5096(02)00025-X.

[61] J. C. Weaver *et al.*, "Unifying design strategies in demosponge and hexactinellid skeletal systems," *J. Adhes.*, vol. 86, no. 1, pp. 72–95, 2010, doi: 10.1080/00218460903417917.

[62] A. Miserez *et al.*, "Effects of laminate architecture on fracture resistance of sponge biosilica: Lessons from nature," *Adv. Funct. Mater.*, vol. 18, no. 8, pp. 1241–1248, 2008, doi: 10.1002/adfm.200701135.

[63] P. Fratzl *et al.*, "Hindered crack propagation in materials with periodically varying young's modulus - Lessons from biological materials," *Adv. Mater.*, vol. 19, no. 18, pp. 2657–2661, 2007, doi: 10.1002/adma.200602394.

[64] F. D. Fischer, O. Kolednik, J. Predan, H. Razi, and P. Fratzl, "Crack driving force in twisted plywood structures," *Acta Biomater.*, vol. 55, pp. 349–359, 2017, doi: 10.1016/j.actbio.2017.04.007.

[65] A. R. Studart, "Additive manufacturing of biologically-inspired materials," *Chem. Soc. Rev.*, vol. 45, pp. 359–376, 2016, doi: 10.1039/C5CS00836K.

[66] Z. Xia, "Wear-resistant and Impact-resistant Materials," in *Biomimetic Principles and Design of Advanced Engineering Materials*, 1st ed., Chichester (UK): John Wiley & Sons Ltd., 2016, pp. 49–78.

[67] Y. Chang and P. Y. Chen, "Hierarchical structure and mechanical properties of snake (Naja atra) and turtle (Ocadia sinensis) eggshells," *Acta Biomater.*, vol. 31, pp. 33–49, 2016, doi: 10.1016/j.actbio.2015.11.040.

[68] A. P. Jackson, J. F. V. Vincent, and R. M. Turner, "The mechanical design of nacre," *Proc. R. Soc. London*, vol. B234, pp. 415–440, 1988, doi: 10.1098/rspb.1988.0056.

[69] S. Deville, E. Saiz, R. K. Nalla, and A. p. Tomsia, "Freezing as a Path to Build Complex Composites," *Science (80-. ).*, vol. 311, pp. 515–518, 2006, doi: 10.1126/science.1120937.

[70] L. K. Grunenfelder *et al.*, "Bio-inspired impact-resistant composites," *Acta Biomater.*, vol. 10, no. 9, pp. 3997–4008, 2014, doi: 10.1016/j.actbio.2014.03.022.

[71] F. Libonati, G. X. Gu, Z. Qin, L. Vergani, and M. J. Buehler, "Bone-Inspired Materials by Design: Toughness Amplification Observed Using 3D Printing and Testing," *Adv. Eng. Mater.*, vol. 18, no. 8, pp. 1354–1363, 2016, doi: 10.1002/adem.201600143.

[72] H. Zhao *et al.*, "Cloning Nacre's 3D Interlocking Skeleton in Engineering Composites to Achieve Exceptional Mechanical Properties," *Adv. Mater.*, vol. 28, pp. 5099–5105, 2016, doi: 10.1002/adma.201600839.

[73] H. Bai *et al.*, "Bioinspired Hydroxyapatite/Poly(methyl methacrylate) Composite with a Nacre-Mimetic Architecture by a Bidirectional Freezing Method," *Adv. Mater.*, vol. 28, pp. 50–56, 2016, doi: 10.1002/adma.201504313.

[74] P. Liu, D. Zhu, Y. Yao, J. Wang, and T. Q. Bui, "Numerical simulation of ballistic impact behavior of bio-inspired scale-like protection system," *Mater. Des.*, vol. 99, pp. 201–210, 2016, doi: 10.1016/j.matdes.2016.03.040.

[75] E. Lin, Y. Li, J. C. Weaver, C. Ortiz, and M. C. Boyce, "Tunability and enhancement of mechanical behavior with additively manufactured bio-inspired hierarchical suture interfaces," *J. Mater. Res.*, vol. 29, no. 17, pp. 1867–1875, 2014, doi: 10.1557/jmr.2014.175.

[76] O. Kolednik, J. Predan, F. D. Fischer, and P. Fratzl, "Bioinspired design criteria for damage-resistant materials with periodically varying microstructure," *Adv. Funct. Mater.*, vol. 21, no. 19, pp. 3634–3641, 2011, doi: 10.1002/adfm.201100443.

[77] M. E. Launey, P. Y. Chen, J. McKittrick, and R. O. Ritchie, "Mechanistic aspects of the fracture toughness of elk antler bone," *Acta Biomater.*, vol. 6, no. 4, pp. 1505–1514, 2010, doi: 10.1016/j.actbio.2009.11.026.

[78] V. Imbeni, J. J. Kruzic, G. W. Marshall, S. J. Marshall, and R. O. Ritchie, "The dentin-enamel junction and the fracture of human teeth," *Nat. Mater.*, vol. 4, no. 3, pp. 229–232, 2005, doi: 10.1038/nmat1323.

[79] L. A. Burns, "Tree joints: Biomimetic insights for aerospace composite joints," in *27th Congress of the International Council of the Aeronautical Sciences 2010, ICAS 2010*, 2010, vol. 3, pp. 1979–1988.

[80] G. X. Gu, M. Takaffoli, A. J. Hsieh, and M. J. Buehler, "Biomimetic additive manufactured polymer composites for improved impact resistance," *Extrem. Mech. Lett.*, vol. 9, pp. 317–323, 2016, doi: 10.1016/j.eml.2016.09.006.

[81] J. J. Kruzic, R. K. Nalla, J. H. Kinney, and R. O. Ritchie, "Crack blunting, crack bridging and resistance-curve fracture mechanics in dentin: Effect of hydration," *Biomaterials*, vol. 24, no. 28, pp. 5209–5221, 2003, doi: 10.1016/S0142-9612(03)00458-7.

[82] B. Kahler, M. V Swain, and A. Moule, "Fracture-toughening mechanisms responsible for differences in work to fracture of hydrated and dehydrated dentine," *J. Biomech.*, vol. 36, no. 2, pp. 229–237, 2003, doi: 10.1016/S0021-9290(02)00327-5.

[83] S. Weiner and H. D. Wagner, "THE MATERIAL BONE : Structure-Mechanical Function Relations," 1998.

[84] H. D. Wagner and S. Weiner, "On the relationship between the microstructure of bone and its mechanical stiffness," *J. Biomech.*, vol. 25, no. 11, pp. 1311–1320, 1992, doi: 10.1016/0021-9290(92)90286-A.

[85] S. Weiner, W. Traub, and H. D. Wagner, "Lamellar bone: Structure-function relations," *J. Struct. Biol.*,

vol. 126, no. 3, pp. 241–255, 1999, doi: 10.1006/jsbi.1999.4107.

[86] E. P. Katz and S. T. Li, "Structure and function of bone collagen fibrils," *J. Mol. Biol.*, vol. 80, no. 1, pp. 1–15, 1973, doi: 10.1016/0022-2836(73)90230-1.

[87] J. L. Katz, "Anisotropy of Young's modulus of bone," *Nature*, vol. 283, no. 5742. pp. 106–107, 1980, doi: 10.1038/283106a0.

[88] W. Bonfield and M. D. Grynpas, "Anisotropy of the Young's modulus of bone," *Nature*, vol. 270, no. 5636, pp. 453–454, 1977, doi: 10.1038/270453a0.

[89] E. D. Yilmaz, G. A. Schneider, and M. V. Swain, "Influence of structural hierarchy on the fracture behaviour of tooth enamel," *Philosophical Transactions of the Royal Society A: Mathematical, Physical and Engineering Sciences*, vol. 373, no. 2038. 2015, doi: 10.1098/rsta.2014.0130.

[90] L. E. Bertassoni, "Dentin on the nanoscale: Hierarchical organization, mechanical behavior and bioinspired engineering," *Dental Materials*, vol. 33, no. 6. pp. 637–649, 2017, doi: 10.1016/j.dental.2017.03.008.

[91] J. J. Martin, B. E. Fiore, and R. M. Erb, "Designing bioinspired composite reinforcement architectures via 3D magnetic printing," *Nat. Commun.*, vol. 6, pp. 1–7, 2015, doi: 10.1038/ncomms9641.

[92] V. Naglieri, B. Gludovatz, A. P. Tomsia, and R. O. Ritchie, "Developing strength and toughness in bio-inspired silicon carbide hybrid materials containing a compliant phase," *Acta Mater.*, vol. 98, pp. 141–151, 2015, doi: 10.1016/j.actamat.2015.07.022.

[93] S. Wang, X. Zhu, X. Yan, J. Deng, R. Wang, and X. Wang, "Nanostructured individual nacre tablet: a subtle designed organic–inorganic composite," *CrystEngComm*, vol. 17, pp. 2964–2968, 2015, doi: 10.1039/C4CE02308K.

[94] J. J. Wang, J. Qiao, J. J. Wang, Y. Zhu, and L. Jiang, "Bioinspired hierarchical alumina-graphene oxide-poly(vinyl alcohol) artificial nacre with optimized strength and toughness," *ACS Appl. Mater. Interfaces*, vol. 7, pp. 9281–9286, 2015, doi: 10.1021/acsami.5b02194.

[95] P. Zhang, M. A. Heyne, and A. C. To, "Biomimetic staggered composites with highly enhanced energy dissipation: Modeling, 3D printing, and testing," *J. Mech. Phys. Solids*, vol. 83, no. November 2016, pp. 285–300, 2015, doi: 10.1016/j.jmps.2015.06.015.

[96] K. Chen, B. Shi, Y. Yue, J. Qi, and L. Guo, "Binary Synergy Strengthening and Toughening of Bio-Inspired Nacre-like Graphene Oxide/Sodium Alginate Composite Paper," *ACS Nano*, vol. 9, no. 8, pp. 8165–8175, 2015, doi: 10.1021/acsnano.5b02333.

[97] J. Wang, Q. Cheng, L. Lin, and L. Jiang, "Synergistic toughening of bioinspired poly(vinyl alcohol)-clay-nanofibrillar cellulose artificial nacre," *ACS Nano*, vol. 8, no. 3, pp. 2739–2745, 2014, doi: 10.1021/nn406428n.

[98] H. F. Tan, B. Zhang, J. W. Yan, X. D. Sun, and G. P. Zhang, "Synthesis and toughening behavior of bio-inspired nanocrystalline TiO 2 / polyelectrolyte nanolayered composites," *Mater. Res. Bull.*, vol. 50, pp. 128–131, 2014, doi: 10.1016/j.materresbull.2013.10.019.

[99] S. Huang, S. L. Phua, W. Liu, G. Ding, and X. Lu, "Nacre-like composite films based on mussel-inspired 'glue' and nanoclay," *RSC Adv.*, vol. 4, pp. 1425–1431, 2014, doi: 10.1039/c3ra45793a.

[100] W. Cui *et al.*, "A Strong Integrated Strength and Toughness Artificial Nacre Based on Dopamine Cross-Linked Graphene Oxide," *ACS Nano*, vol. 8, no. 9, pp. 9511–9517, 2014, doi: 10.1021/nn503755c.

[101] H. Humburg, E. Volkmann, D. Koch, and J. Müssig, "Combination of biological mechanisms for a concept study of a fracture-tolerant bio-inspired ceramic composite material," *J. Mater. Sci.*, vol. 49, no. 23, pp. 8040–8050, 2014, doi: 10.1007/s10853-014-8511-x.

[102] Q. Cheng, M. Wu, and L. Jiang, "Ultratough artificial nacre based on conjugated cross-linked graphene oxide," in *Technical Proceedings of the 2013 NSTI Nanotechnology Conference and Expo, NSTI-Nanotech 2013*, 2013, vol. 1, pp. 231–234, doi: 10.1002/ange.201301081.

[103] J. Wang, Q. Cheng, L. Lin, L. Chen, and L. Jiang, "Understanding the relationship of performance with nanofiller content in the biomimetic layered nanocomposites," *Nanoscale*, vol. 5, no. 14, pp. 6356–6362, 2013, doi: 10.1039/c3nr00801k.

[104] L. S. Dimas and M. J. Buehler, “Influence of geometry on mechanical properties of bio-inspired silica-based hierarchical materials,” *Bioinspiration and Biomimetics*, vol. 7, no. 3, 2012, doi: 10.1088/1748-3182/7/3/036024.

[105] H. Humburg, D. Zhu, S. Beznia, and F. Barthelat, “Bio-inspired tapered fibers for composites with superior toughness,” *Compos. Sci. Technol.*, vol. 72, no. 9, pp. 1012–1019, 2012, doi: 10.1016/j.compscitech.2012.03.013.

[106] Y. Q. Li, T. Yu, T. Y. Yang, L. X. Zheng, and K. Liao, “Bio-Inspired nacre-like composite films based on graphene with superior mechanical, electrical, and biocompatible properties,” *Adv. Mater.*, vol. 24, pp. 3426–3431, 2012, doi: 10.1002/adma.201200452.

[107] Q. Cheng, M. Li, L. Jiang, and Z. Tang, “Bioinspired layered composites based on flattened double-walled carbon nanotubes,” *Adv. Mater.*, vol. 24, no. 14, pp. 1838–1843, 2012, doi: 10.1002/adma.201200179.

[108] Z. Burghard, L. Zini, V. Srot, P. Bellina, P. A. Van Aken, and J. Bill, “Toughening through nature-adapted nanoscale design,” *Nano Lett.*, vol. 9, no. 12, pp. 4103–4108, 2009, doi: 10.1021/nl902324x.

[109] C. an Wang, Y. Huang, Q. Zan, H. Guo, and S. Cai, “Biomimetic structure design - a possible approach to change the brittleness of ceramics in nature,” in *Materials Science and Engineering C*, 2000, vol. 11, no. 1, pp. 9–12, doi: 10.1016/S0928-4931(00)00133-8.

[110] Q. L. Feng, F. Z. Cui, G. Pu, R. Z. Wang, and H. D. Li, “Crystal orientation, toughening mechanisms and a mimic of nacre,” *Mater. Sci. Eng. C*, vol. 11, no. 1, pp. 19–25, 2000, doi: 10.1016/S0928-4931(00)00138-7.

[111] F. Barthelat and D. Zhu, “A novel biomimetic material duplicating the structure and mechanics of natural nacre,” *J. Mater. Res.*, vol. 26, no. 10, pp. 1203–1215, 2011, doi: 10.1557/jmr.2011.65.

[112] S. Wan, J. Peng, L. Jiang, and Q. Cheng, “Bioinspired Graphene-Based Nanocomposites and Their Application in Flexible Energy Devices,” *Adv. Mater.*, vol. 28, no. 36, pp. 7862–7898, 2016, doi: 10.1002/adma.201601934.

[113] D. B. Xiong *et al.*, “Graphene-and-Copper Artificial Nacre Fabricated by a Preform Impregnation Process: Bioinspired Strategy for Strengthening-Toughening of Metal Matrix Composite,” *ACS Nano*, vol. 9, no. 7, pp. 6934–6943, 2015, doi: 10.1021/acsnano.5b01067.

[114] C. Hu, L. Zhang, and M. Wei, “Development of Biomimetic Scaffolds with Both Intrafibrillar and Extrafibrillar Mineralization,” *ACS Biomater. Sci. Eng.*, vol. 1, pp. 669–676, 2015, doi: 10.1021/acsbiomaterials.5b00088.

[115] L. S. Dimas, G. H. Bratzel, I. Eylon, and M. J. Buehler, “Tough Composites Inspired by Mineralized Natural Materials : Computation , 3D printing , and Testing,” *Adv. Funct. Mater.*, vol. 23, no. 36, pp. 4629–4638, 2013, doi: 10.1002/adfm.201300215.

[116] C. Li, A. K. Born, T. Schweizer, M. Zenobi-Wong, M. Cerruti, and R. Mezzenga, “Amyloid-hydroxyapatite bone biomimetic composites,” *Adv. Mater.*, vol. 26, pp. 3207–3212, 2014, doi: 10.1002/adma.201306198.

[117] C. Zhu *et al.*, “Novel polypropylene biocomposites reinforced with carbon nanotubes and hydroxyapatite nanorods for bone replacements,” *Mater. Sci. Eng. C*, vol. 33, no. 3, pp. 1380–1388, 2013, doi: 10.1016/j.msec.2012.12.039.

[118] U. S. Shin, I. K. Yoon, G. S. Lee, W. C. Jang, J. C. Knowles, and H. W. Kim, “Carbon nanotubes in nanocomposites and hybrids with hydroxyapatite for bone replacements,” *Journal of Tissue Engineering*, vol. 2, no. 1. pp. 1–10, 2011, doi: 10.4061/2011/674287.

[119] G. Pezzotti, S. M. F. Asmus, L. P. Ferroni, and S. Miki, “In situ polymerization into porous ceramics: A novel route to tough biomimetic materials,” *J. Mater. Sci. Mater. Med.*, vol. 13, no. 8, pp. 783–787, 2002, doi: 10.1023/A:1016127209117.

[120] B. Chen, X. Peng, J. G. Wang, and X. Wu, “Laminated microstructure of Bivalva shell and research of biomimetic ceramic/polymer composite,” in *Ceramics International*, 2004, vol. 30, no. 7, pp. 2011–2014, doi: 10.1016/j.ceramint.2003.12.169.

[121] A. J. Goetz *et al.*, “Interdigitating biocalcite dendrites form a 3-D jigsaw structure in brachiopod shells,” *Acta Biomater.*, vol. 7, pp. 2237–2243, 2011, doi: 10.1016/j.actbio.2011.01.035.

[122] A. M. Beese, Z. An, S. Sarkar, S. S. P. Nathamgari, H. D. Espinosa, and S. T. Nguyen, “Defect-tolerant nanocomposites through bio-inspired stiffness modulation,” *Adv. Funct. Mater.*, vol. 24, no. 19, pp. 2883–2891, 2014, doi: 10.1002/adfm.201303503.

[123] I. Zlotnikov *et al.*, “In situ elastic modulus measurements of ultrathin protein-rich organic layers in biosilica: Towards deeper understanding of superior resistance to fracture of biocomposites,” *RSC Adv.*, vol. 3, no. 17, pp. 5798–5802, 2013, doi: 10.1039/c3ra40574e.

[124] S. L. Walter, B. D. Flinn, and G. Mayer, “Mechanisms of toughening of a natural rigid composite,” *Mater. Sci. Eng. C*, vol. 27, no. 3, pp. 570–574, 2007, doi: 10.1016/j.msec.2006.05.020.

[125] G. Mayer, “Rigid Biological Systems as Models for Synthetic Composites,” *Science (80-. ).*, vol. 310, pp. 1144–1147, 2005, doi: 10.1126/science.1116994.

[126] R. Merindol, S. Diabang, O. Felix, T. Roland, C. Gauthier, and G. Decher, “Bio-Inspired Multiproperty Materials: Strong, Self-Healing, and Transparent Artificial Wood Nanostructures,” *ACS Nano*, vol. 9, no. 2, pp. 1127–1136, 2015, doi: 10.1021/nn504334u.

[127] L. Burns, A. P. Mouritz, D. Pook, and S. Feih, “Bio-inspired hierarchical design of composite T-joints with improved structural properties,” *Compos. Part B Eng.*, vol. 69, pp. 222–231, 2015, doi: 10.1016/j.compositesb.2014.09.041.

[128] B. G. Compton and J. A. Lewis, “3D-printing of lightweight cellular composites,” *Adv. Mater.*, vol. 26, no. 34, pp. 5930–5935, 2014, doi: 10.1002/adma.201401804.

[129] S. Klaithong, D. Van Opdenbosch, C. Zollfrank, and J. Plank, “Preparation of CaCO3 and CaO replicas retaining the hierarchical structure of spruce wood,” *Zeitschrift fur Naturforsch. - Sect. B J. Chem. Sci.*, vol. 68, no. 5–6, pp. 533–538, 2013, doi: 10.5560/ZNB.2013-3062.

[130] H. Sehaqui, Q. Zhou, and L. a. Berglund, “Nanostructured biocomposites of high toughness—a wood cellulose nanofiber network in ductile hydroxyethylcellulose matrix,” *Soft Matter*, vol. 7, pp. 7342–7350, 2011, doi: 10.1039/c1sm05325f.

[131] T. Huber, N. Graupner, and J. Müssig, “As tough as it is delicious? A mechanical and structural analysis of red rhubarb (Rheum rhabarbarum),” *J. Mater. Sci.*, vol. 44, pp. 4195–4199, 2009, doi: 10.1007/s10853-009-3556-y.

[132] A. P. Garcia, N. Pugno, and M. J. Buehler, “Superductile, wavy silica nanostructures inspired by diatom algae,” *Adv. Eng. Mater.*, vol. 13, no. 10, pp. 405–414, 2011, doi: 10.1002/adem.201080113.

[133] Y. Wenbo, K. Zhu, Y. Aman, Z. Guo, and S. Xiong, “Bio-inspired design of SiCf-reinforced multi-layered Ti-intermetallic composite,” *Mater. Des.*, vol. 101, pp. 102–108, 2016, doi: 10.1016/j.matdes.2016.03.138.

[134] D. Verma, T. Qu, and V. Tomar, “Scale Dependence of the Mechanical Properties and Microstructure of Crustaceans Thin Films as Biomimetic Materials,” *JOM*, vol. 67, no. 4. pp. 858–866, 2015, doi: 10.1007/s11837-015-1337-4.

[135] X. Li *et al.*, “Spear and Shield: Survival War between Mantis Shrimps and Abalones,” *Adv. Mater. Interfaces*, vol. 2, no. 14, pp. 1–5, 2015, doi: 10.1002/admi.201500250.

[136] L. K. Grunenfelder, S. Herrera, and D. Kisailus, “Crustacean-derived biomimetic components and nanostructured composites,” *Small*, vol. 10, no. 16. pp. 3207–3232, 2014, doi: 10.1002/smll.201400559.

[137] G. W. Milliron, “Lightweight Impact-Resistant Composite Materials : Lessons from Mantis Shrimp (Dissertation: Doctor of Philosophy),” University of California Riverside, 2012.

[138] L. Chen, R. Ballarini, H. Kahn, and A. H. Heuer, “Bioinspired micro-composite structure,” *J. Mater. Res.*, vol. 22, no. 1, pp. 124–131, 2007.

[139] C. Hedegaard, “Shell structures of the recent Vetigastropoda,” in *Journal of Molluscan Studies*, 1997, vol. 63, no. 3, pp. 369–377, doi: 10.1093/mollus/63.3.369.

[140] J. Cheng, D. Park, Y. Jun, J. Lee, J. Hyun, and S.-H. Lee, “Biomimetic Spinning of Silk Fibers and in situ Cell Encapsulation,” *Lab Chip*, vol. 16, pp. 2654–2661, 2016, doi: 10.1039/C6LC00488A.

[141] L. Huang, C. Li, W. Yuan, and G. Shi, “Strong composite films with layered structures prepared by casting silk fibroin-graphene oxide hydrogels,” *Nanoscale*, vol. 5, no. 9, pp. 3780–3786, 2013, doi:

10.1039/C3NR00196B.

[142] M. Elices *et al.*, "Bioinspired fibers follow the track of natural spider silk," *Macromolecules*, vol. 44, pp. 1166–1176, 2011, doi: 10.1021/ma102291m.

[143] C. Fu, Z. Shao, and V. Fritz, "Animal silks: Their structures, properties and artificial production," *Chemical Communications*, no. 43. pp. 6515–6529, 2009, doi: 10.1039/b911049f.

[144] P. Papadopoulos, J. Solter, and F. Kremer, "Hierarchies in the structural organization of spider silk-a quantitative model," *Colloid Polym. Sci.*, vol. 287, pp. 231–236, 2009, doi: 10.1007/s00396-008-1968-x.

[145] S. Keten and M. J. Buehler, "Geometric confinement governs the rupture strength of h-bond assemblies at a critical length scale," *Nano Lett.*, vol. 8, no. 2, pp. 743–748, 2008, doi: 10.1021/nl0731670.

[146] J. Xiao and S. Yang, "Biomimetic synthesis, hierarchical assembly and mechanical properties of calcite/chitosan composites in a three-dimensional chitosan scaffold," *Adv. Eng. Mater.*, vol. 13, no. 1–2, pp. 32–40, 2011, doi: 10.1002/adem.201080068.

[147] B. Chen, X. Peng, C. Cai, H. Niu, and X. Wu, "Helicoidal microstructure of Scarabaei cuticle and biomimetic research," *Mater. Sci. Eng. A*, vol. 423, no. 1–2, pp. 237–242, 2006, doi: 10.1016/j.msea.2005.11.069.

[148] B. Chen and J. Fan, "Microstructures of chafer cuticle and biomimetic design," in *Journal of Computer-Aided Materials Design*, 2005, vol. 11, no. 2–3, pp. 201–210, doi: 10.1007/s10820-005-3174-1.

[149] Z. Yu and D. Lau, "Molecular dynamics study on stiffness and ductility in chitin–protein composite," *J. Mater. Sci.*, vol. 50, no. 21, pp. 7149–7157, 2015, doi: 10.1007/s10853-015-9271-y.

[150] J. M. Malho *et al.*, "Formation of ceramophilic chitin and biohybrid materials enabled by a genetically engineered bifunctional protein," *Chem Commun*, vol. 50, pp. 7348–7351, 2014, doi: 10.1039/c4cc02170c.

[151] J. Plocher and A. Panesar, "Review on design and structural optimisation in additive manufacturing: Towards next-generation lightweight structures," *Mater. Des.*, vol. 183, p. 108164, 2019, doi: 10.1016/j.matdes.2019.108164.

[152] A. K. Rajasekharan, R. Bordes, C. Sandström, and M. Ekh, "Hierarchical and Heterogeneous Bioinspired Composites — Merging Molecular Self-Assembly with Additive Manufacturing," *Small*, vol. 13, no. 1700550, pp. 1–11, 2017, doi: 10.1002/smll.201700550.

[153] B. Felbrich *et al.*, "A novel rapid additive manufacturing concept for architectural composite shell construction inspired by the shell formation in land snails," *Bioinspiration and Biomimetics*, vol. 13, no. 2, 2018, doi: 10.1088/1748-3190/aaa50d.

[154] T. Kamps, M. Gralow, G. Schlick, and G. Reinhart, "Systematic Biomimetic Part Design for Additive Manufacturing," *Procedia CIRP*, vol. 65, pp. 259–266, 2017, doi: 10.1016/j.procir.2017.04.054.

[155] J. Plocher, C. Lee, and A. Panesar, "Additve Manufacturing of Bone-Inspired Structural Power Composites," 2019.

[156] R. M. Erb, R. Libanori, and N. Rothfuchs, "Composites Reinforced in Three Dimensions by Using Low Magnetic Fields," *Science (80-. ).*, vol. 335, pp. 199–204, 2012, doi: 10.1126/science.1210822.

[157] M. Grossman, F. Bouville, F. Erni, K. Masania, R. Libanori, and A. R. Studart, "Mineral Nano-Interconnectivity Stiffens and Toughens Nacre-like Composite Materials," *Adv. Mater.*, vol. 29, no. 8, 2017, doi: 10.1002/adma.201605039.

[158] E. Feilden *et al.*, "3D Printing Bioinspired Ceramic Composites," *Sci. Rep.*, vol. 7, no. 1, pp. 1–9, 2017, doi: 10.1038/s41598-017-14236-9.

[159] T. H. Lin, W. H. Huang, I. K. Jun, and P. Jiang, "Bioinspired assembly of surface-roughened nanoplatelets," *J. Colloid Interface Sci.*, vol. 344, no. 2, pp. 272–278, 2010, doi: 10.1016/j.jcis.2009.12.060.

[160] S. V. Mirkhalaf and F. Barthelat, "A laser-engraved glass duplicating the structure, mechanics and performance of natural nacre," *Bioinspir. Biomim.*, vol. 10, no. 2, p. 026005, 2015, doi: 10.1088/1748-3190/10/2/026005.

[161] F. Narducci and S. T. Pinho, "Exploiting nacre-inspired crack deflection mechanisms in CFRP via micro-

structural design," *Compos. Sci. Technol.*, vol. 153, pp. 178–189, 2017, doi: 10.1016/j.compscitech.2017.08.023.

[162] F. Narducci and S. T. Pinho, "Interaction between nacre-like CFRP mesolayers and long-fibre interlayers," *Compos. Struct.*, vol. 200, pp. 921–928, 2018, doi: 10.1016/j.compstruct.2018.05.103.

[163] F. Narducci, K.-Y. Lee, and S. T. Pinho, "Realising damage-tolerant nacre-inspired CFRP," *J. Mech. Phys. Solids*, vol. 116, pp. 391–402, 2018, doi: 10.1016/j.jmps.2018.04.004.

[164] J. A. Pascoe, S. Pimenta, and S. T. Pinho, "TiGr-nacre: A new damage-tolerant composite," 2019.

[165] R. Häsä and S. T. Pinho, "Failure mechanisms of biological crossed-lamellar microstructures applied to synthetic high-performance fibre-reinforced composites," *J. Mech. Phys. Solids*, vol. 125, pp. 53–73, 2019, doi: 10.1016/j.jmps.2018.12.008.

[166] R. Häsä and S. T. Pinho, "A three-level hybrid metal/in-plane-CFRP/crossed-lamellar microstructure concept for containment applications," *Compos. Part A Appl. Sci. Manuf.*, vol. 126, p. 105609, 2019, doi: 10.1016/j.compositesa.2019.105609.

[167] R. Häsä and S. T. Pinho, "A novel aluminium/CFRP hybrid composite with a bio-inspired crossed-lamellar microstructure for preservation of structural integrity," *Compos. Sci. Technol.*, vol. 182, p. 107760, 2019, doi: 10.1016/j.compscitech.2019.107760.

[168] R. Menig, M. A. H. Meyers, M. A. H. Meyers, and K. S. Vecchio, "Quasi-static and dynamic mechanical response of Strombus gigas (conch) shells," *Mater. Sci. Eng. A*, vol. 297, pp. 203–211, 2001, doi: http://dx.doi.org/10.1016/S0921-5093(00)01228-4.

[169] S. Dipette, A. Ural, and S. Santhanam, "Analysis of toughening mechanisms in the Strombus gigas shell," *J. Mech. Behav. Biomed. Mater.*, vol. 48, pp. 200–209, 2015, doi: 10.1016/j.jmbbm.2015.04.011.

[170] H. Zell and P. Whiskey, "Eustrombus gigas," 2010. https://commons.wikimedia.org/wiki/File:Lobatus_gigas_01.jpg (accessed Apr. 30, 2020).

[171] M. Yourdkhani, D. Pasini, and F. Barthelat, "Multiscale mechanics and optimization of gastropod shells," *J. Bionic Eng.*, vol. 8, no. 4, pp. 357–368, 2011, doi: 10.1016/S1672-6529(11)60041-3.

[172] F. Barthelat, "Biological materials by design Nacre from mollusk shells : a model for high-performance structural materials," *Bioinspir. Biomim.*, vol. 5, no. 035001, pp. 1–8, 2010, doi: 10.1088/1748-3182/5/3/035001.

[173] M. A. Meyers, P.-Y. Y. Chen, M. I. Lopez, Y. Seki, and A. Y. M. M. Lin, *Biological materials: A materials science approach*, vol. 4, no. 5. Elsevier Ltd, 2011, pp. 626–657.

[174] R. Z. Wang, Z. Suo, A. G. Evans, N. Yao, and I. A. Aksay, "Deformation mechanisms in nacre," *J. Mater. Res.*, vol. 16, pp. 2485–2493, 2001, doi: https://doi.org/10.1557/JMR.2001.0340.

[175] G. M. Luz and J. F. Mano, "Nacre-Inspired Biomaterials," in *Biomimetic Approaches for Biomaterials Development*, 2012, pp. 313–331.

[176] C. Wang, B. Long, W. Lin, Y. Huang, and J. Sun, "Poly (amic acid)– clay nacrelike composites prepared by electrophoretic deposition," *J. Mater. Res.*, vol. 23, no. 6, pp. 1706–1712, 2008, doi: 10.1557/JMR.2008.0209.

[177] B. Long and C. Wang, "Polyacrylamide-clay nacre-like nanocomposites prepared by electrophoretic deposition," *Compos. Sci. Technol.*, vol. 67, pp. 2770–2774, 2007, doi: 10.1016/j.compscitech.2007.02.007.

[178] W. Lin, C. an Wang, H. Le, B. Long, and Y. Huang, "Special assembly of laminated nanocomposite that mimics nacre," *Mater. Sci. Eng. C*, vol. 28, no. 7, pp. 1031–1037, 2008, doi: 10.1016/j.msec.2007.04.030.

[179] M. Mirkhalaf, a K. Dastjerdi, and F. Barthelat, "Overcoming the brittleness of glass through bio-inspiration and micro-architecture," *Nat. Commun.*, vol. 5, p. 3166, 2014, doi: 10.1038/ncomms4166.

[180] C. Huang and Q. Cheng, "Learning from nacre: Constructing polymer nanocomposites," *Composites Science and Technology*, vol. 150. pp. 141–166, 2017, doi: 10.1016/j.compscitech.2017.07.021.

[181] R. Malkin, M. Yasaee, R. S. Trask, and I. P. Bond, "Bio-inspired laminate design exhibiting pseudo-ductile (graceful) failure during flexural loading," *Compos. Part A Appl. Sci. Manuf.*, vol. 54, pp. 107–116, 2013, doi: 10.1016/j.compositesa.2013.07.008.

[182] S. Pimenta and P. Robinson, “An analytical shear-lag model for composites with ‘brick-and-mortar’ architecture considering non-linear matrix response and failure,” *Compos. Sci. Technol.*, vol. 104, pp. 111–124, 2014, doi: 10.1016/j.compscitech.2014.09.001.

[183] G. Czél and M. R. Wisnom, “Demonstration of pseudo-ductility in high performance glass/epoxy composites by hybridisation with thin-ply carbon prepreg,” *Compos. Part A Appl. Sci. Manuf.*, vol. 52, pp. 23–30, 2013, doi: 10.1016/j.compositesa.2013.04.006.

[184] G. Czél, S. Pimenta, M. R. Wisnom, and P. Robinson, “Demonstration of pseudo-ductility in unidirectional discontinuous carbon fibre/epoxy prepreg composites,” *Compos. Sci. Technol.*, vol. 106, pp. 110–119, 2015, doi: 10.1016/j.compscitech.2014.10.022.

[185] J. Henry and S. Pimenta, “Semi-analytical simulation of aligned discontinuous composites,” *Compos. Sci. Technol.*, vol. 144, pp. 230–244, 2017, doi: 10.1016/j.compscitech.2017.01.027.

[186] J. Henry and S. Pimenta, “Modelling hybrid effects on the stiffness of aligned discontinuous composites with hybrid fibre-types,” *Compos. Sci. Technol.*, vol. 152, pp. 275–289, 2017, doi: 10.1016/j.compscitech.2017.08.017.

[187] F. Libonati, A. E. Vellwock, F. Ielmini, D. Abliz, G. Ziegmann, and L. Vergani, “Bone-inspired enhanced fracture toughness of de novo fiber reinforced composites,” *Sci. Rep.*, vol. 9, no. 1, p. 3142, 2019, doi: 10.1038/s41598-019-39030-7.

[188] J. Tang *et al.*, “Discontinuities as a way to influence the failure mechanisms and tensile performance of hybrid carbon fiber/self-reinforced polypropylene composites,” *Compos. Part A Appl. Sci. Manuf.*, vol. 107, pp. 354–365, 2018, doi: 10.1016/j.compositesa.2018.01.020.

[189] J. Tang *et al.*, “Staggered ply discontinuities for tailoring the tensile behavior of hybrid carbon fiber/self-reinforced polypropylene composites: A study of pattern parameters,” *Compos. Part A Appl. Sci. Manuf.*, vol. 125, p. 105551, 2019, doi: 10.1016/j.compositesa.2019.105551.

[190] J. Tang *et al.*, “Engineering tensile behavior of hybrid carbon fiber/self-reinforced polypropylene composites by bio-inspired fiber discontinuities,” *Compos. Part B Eng.*, vol. 178, p. 107502, Dec. 2019, doi: 10.1016/j.compositesb.2019.107502.

[191] L. Mencattelli, J. Tang, Y. Swolfs, L. Gorbatikh, and S. T. Pinho, “Bio-inspired design for enhanced damage tolerance of self-reinforced polypropylene/carbon fibre polypropylene hybrid composites,” *Compos. Part A Appl. Sci. Manuf.*, vol. 121, pp. 341–352, Mar. 2019, doi: 10.1016/j.compositesa.2019.03.028.

[192] R. Rabiei, S. Bekah, and F. Barthelat, “Failure mode transition in nacre and bone-like materials,” *Acta Biomater.*, vol. 6, pp. 4081–4089, 2010, doi: 10.1016/j.actbio.2010.04.008.

[193] R. Lakes, “Materials with structural hierarchy,” *Nature*, vol. 361, pp. 511–515, 1993.

[194] R. Buckwalter, J. A., Glimcher, M. J., Cooper, R. R. & Recker, “Bone Biology: Structure, blood-supply, cells, matrix, and mineralization,” *J. Bone Jt. Surg.*, vol. 77, no. 8, pp. 1256–1275, 1995.

[195] G. Bullegas, S. T. Pinho, and S. Pimenta, “Engineering the translaminar fracture behaviour of thin-ply composites,” *Compos. Sci. Technol.*, vol. 131, pp. 110–122, 2016, doi: 10.1016/j.compscitech.2016.06.002.

[196] G. Bullegas, J. Benoliel, P. L. Fenelli, S. T. Pinho, and S. Pimenta, “Towards quasi isotropic laminates with engineered fracture behaviour for industrial applications,” *Compos. Sci. Technol.*, vol. 165, pp. 290–306, 2018, doi: 10.1016/j.compscitech.2018.07.004.

[197] D. Fengel and G. Wegener, *Wood: chemistry, ultrastructure, reactions*, 1st ed. Berlin: Walter de Gruyter & Co., 1989.

[198] L. Salmén, “Micromechanical understanding of the cell-wall structure,” *Comptes Rendus - Biol.*, vol. 327, no. 9–10, pp. 873–880, 2004, doi: 10.1016/j.crvi.2004.03.010.

[199] S. R. Djafari Petroudy, “Physical and mechanical properties of natural fibers,” in *Advanced High Strength Natural Fibre Composites in Construction*, 2017, pp. 59–83.

[200] A. K. Mohanty, M. Misra, L. T. Drzal, S. E. Selke, B. R. Harte, and G. Hinrichsen, “Natural fibers, biopolymers, and biocomposites: An introduction,” in *Natural Fibers, Biopolymers, and Biocomposites*, 2005.

[201] A. Bourmaud, C. Morvan, A. Bouali, V. Placet, P. Perré, and C. Baley, “Relationships between microfibrillar angle, mechanical properties and biochemical composition of flax fibers,” *Ind. Crops Prod.*, vol. 44, pp. 343–351, 2013, doi: 10.1016/j.indcrop.2012.11.031.

[202] I. Burgert, “Exploring the micromechanical design of plant cell walls,” *American Journal of Botany*, vol. 93, no. 10. pp. 1391–1401, 2006, doi: 10.3732/ajb.93.10.1391.

[203] L. J. Gibson, “The hierarchical structure and mechanics of plant materials,” *Journal of the Royal Society Interface*, vol. 9, no. 76. pp. 2749–2766, 2012, doi: 10.1098/rsif.2012.0341.

[204] L. Zorzetto and D. Ruffoni, “Wood-Inspired 3D-Printed Helical Composites with Tunable and Enhanced Mechanical Performance,” *Adv. Funct. Mater.*, vol. 29, no. 1, 2019, doi: 10.1002/adfm.201805888.

[205] K. G. Nair, A. Dufresne, A. Gandini, and M. N. Belgacem, “Crab shell chitin whiskers reinforced natural rubber nanocomposites. 3. Effect of Chemical Modification of chitin whiskers,” *Biomacromolecules*, vol. 4, no. 6, pp. 1835–1842, 2003, doi: 10.1021/bm030058g.

[206] S. L. Gunderson and J. A. Lute, “The Use of Preformed Holes for Increased Strength and Damage Tolerance of Advanced Composites,” *J. Reinf. Plast. Compos.*, vol. 12, no. 5, pp. 559–569, 1993, doi: 10.1177/073168449301200506.

[207] T. Apichattrabrut and K. Ravi-Chandar, “Helicoidal composites,” *Mech. Adv. Mater. Struct.*, vol. 13, no. 1, pp. 61–76, 2006, doi: 10.1080/15376490500343808.

[208] L. Cheng, A. Thomas, J. L. Glancey, and A. M. Karlsson, “Mechanical behavior of bio-inspired laminated composites,” *Compos. Part A Appl. Sci. Manuf.*, vol. 42, no. 2, pp. 211–220, 2011, doi: 10.1016/j.compositesa.2010.11.009.

[209] J. S. Shang, N. H. H. Ngern, and V. B. C. Tan, “Crustacean-inspired helicoidal laminates,” *Compos. Sci. Technol.*, vol. 128, pp. 222–232, 2016, doi: 10.1016/j.compscitech.2016.04.007.

[210] F. Pinto, O. Iervolino, G. Scarselli, D. Ginzburg, and M. Meo, “Bioinspired twisted composites based on Bouligand structures,” in *Proc. SPIE 9797, Bioinspiration, Biomimetics, and Bioreplication 2016*, Apr. 2016, p. 97970E, doi: 10.1117/12.2219088.

[211] D. Ginzburg, F. Pinto, O. Iervolino, and M. Meo, “Damage tolerance of bio-inspired helicoidal composites under low velocity impact,” *Compos. Struct.*, vol. 161, pp. 187–203, 2017, doi: 10.1016/j.compstruct.2016.10.097.

[212] J. L. Liu, H. P. Lee, and V. B. C. Tan, “Failure mechanisms in bioinspired helicoidal laminates,” *Compos. Sci. Technol.*, vol. 157, pp. 99–106, 2018, doi: 10.1016/j.compscitech.2018.01.033.

[213] J. L. Liu, H. P. Lee, and V. B. C. Tan, “Effects of inter-ply angles on the failure mechanisms in bioinspired helicoidal laminates,” *Compos. Sci. Technol.*, vol. 165, pp. 282–289, Sep. 2018, doi: 10.1016/J.COMPSCITECH.2018.07.017.

[214] J. L. Liu, H. P. Lee, S. H. R. Kong, and V. B. C. Tan, “Improving laminates through non-uniform inter-ply angles,” *Compos. Part A Appl. Sci. Manuf.*, vol. 127, p. 105625, Dec. 2019, doi: 10.1016/J.COMPOSITESA.2019.105625.

[215] J. L. Liu, H. P. Lee, K. S. Lai, and V. B. C. Tan, “Bio-Inspired Laminates of Different Material Systems,” *J. Appl. Mech.*, vol. 87, no. March, pp. 1–7, 2020, doi: 10.1115/1.4045280.

[216] J. L. Liu, H. P. Lee, T. E. Tay, and V. B. C. Tan, “Healable bio-inspired helicoidal laminates,” *Compos. Part A Appl. Sci. Manuf.*, vol. 137, p. 106024, 2020, doi: https://doi.org/10.1016/j.compositesa.2020.106024.

[217] L. Mencattelli and S. T. Pinho, “Realising bio-inspired impact damage-tolerant thin-ply CFRP Bouligand structures via promoting diffused sub-critical helicoidal damage,” *Compos. Sci. Technol.*, vol. 182, p. 107684, Jun. 2019, doi: 10.1016/J.COMPSCITECH.2019.107684.

[218] L. Mencattelli and S. T. Pinho, “Ultra-thin-ply CFRP Bouligand bio-inspired structures with enhanced load-bearing capacity, delayed catastrophic failure and high energy dissipation capability,” *Compos. Part A Appl. Sci. Manuf.*, vol. 129, p. 105655, Oct. 2019, doi: 10.1016/J.COMPOSITESA.2019.105655.

[219] L. Mencattelli and S. T. Pinho, “Herringbone-Bouligand CFRP structures: A new tailorable damage-tolerant solution for damage containment and reduced delaminations,” *Compos. Sci. Technol.*, p. 108047, Feb. 2020, doi: 10.1016/J.COMPSCITECH.2020.108047.

[220] M. R. Abir, T. E. Tay, and H. P. Lee, "On the improved ballistic performance of bio-inspired composites," *Compos. Part A Appl. Sci. Manuf.*, vol. 123, pp. 59–70, Aug. 2019, doi: 10.1016/j.compositesa.2019.04.021.

[221] Y. Bouligand, "Twisted fibrous arrangements in biological materials and cholesteric mesophases," *Tissue Cell*, vol. 4, no. 2, pp. 189–217, 1972, doi: 10.1016/S0040-8166(72)80042-9.

[222] J. C. Weaver *et al.*, "The stomatopod dactyl club: A formidable damage-tolerant biological hammer," *Science (80-. ).*, vol. 336, no. 6086, pp. 1275–1280, 2012, doi: 10.1126/science.1218764.

[223] L. Cheng, L. Wang, and A. M. Karlsson, "Image analyses of two crustacean exoskeletons and implications of the exoskeletal microstructure on the mechanical behavior," *J. Mater. Res.*, vol. 23, no. 11, pp. 2854–2872, 2008, doi: 10.1557/JMR.2008.0375.

[224] P. Y. Chen, A. Y. M. Lin, J. McKittrick, and M. A. Meyers, "Structure and mechanical properties of crab exoskeletons," *Acta Biomater.*, vol. 4, no. 3, pp. 587–596, 2008, doi: 10.1016/j.actbio.2007.12.010.

[225] D. Raabe, C. Sachs, and P. Romano, "The crustacean exoskeleton as an example of a structurally and mechanically graded biological nanocomposite material," *Acta Mater.*, vol. 53, no. 15, pp. 4281–4292, 2005, doi: 10.1016/j.actamat.2005.05.027.

[226] D. Raabe *et al.*, "Microstructure and crystallographic texture of the chitin-protein network in the biological composite material of the exoskeleton of the lobster Homarus americanus," *Mater. Sci. Eng. A*, vol. 421, no. 1–2, pp. 143–153, 2006, doi: 10.1016/j.msea.2005.09.115.

[227] A. Al-Sawalmih *et al.*, "Microtexture and chitin/calcite orientation relationship in the mineralized exoskeleton of the american lobster," *Adv. Funct. Mater.*, vol. 18, no. 20, pp. 3307–3314, 2008, doi: 10.1002/adfm.200800520.

[228] L. Cheng, L. Wang, and A. M. Karlsson, "Mechanics-based analysis of selected features of the exoskeletal microstructure of Popillia japonica," *J. Mater. Res.*, vol. 24, no. 11, pp. 3253–3267, 2009, doi: 10.1557/jmr.2009.0409.

[229] R. Yang, A. Zaheri, W. Gao, C. Hayashi, and H. D. Espinosa, "AFM Identification of Beetle Exocuticle: Bouligand Structure and Nanofiber Anisotropic Elastic Properties," *Adv. Funct. Mater.*, vol. 27, no. 6, p. 1603993, Feb. 2017, doi: 10.1002/adfm.201603993.

[230] B. Chen, X. Peng, J. G. Wang, and X. Wu, "Spiry-layup model of Rutelidae cuticle," in *Computational Materials Science*, 2004, vol. 30, no. 3-4 SPEC. ISS., pp. 517–522, doi: 10.1016/j.commatsci.2004.02.045.

[231] S. N. Patek, "Extreme impact and cavitation forces of a biological hammer: strike forces of the peacock mantis shrimp Odontodactylus scyllarus," *J. Exp. Biol.*, vol. 208, no. 19, pp. 3655–3664, 2005, doi: 10.1242/jeb.01831.

[232] N. A. Yaraghi *et al.*, "A Sinusoidally Architected Helicoidal Biocomposite," *Adv. Mater.*, vol. 28, no. 32, pp. 6835–6844, 2016, doi: 10.1002/adma.201600786.

[233] N. Suksangpanya, N. A. Yaraghi, R. B. Pipes, D. Kisailus, and P. Zavattieri, "Crack twisting and toughening strategies in Bouligand architectures," *Int. J. Solids Struct.*, vol. 150, pp. 83–106, 2018, doi: 10.1016/j.ijsolstr.2018.06.004.

[234] K. Ravi-Chandar, "Impact Response of Helicoidal Composites - Final report to the Army Research Office W911NF-05-1-0065, Center for the Mechanics of Solids, Structures and Materials at the University of Texas at Austin," 2011.

[235] P. Murali, T. K. Bhandakkar, W. L. Cheah, M. H. Jhon, H. Gao, and R. Ahluwalia, "Role of modulus mismatch on crack propagation and toughness enhancement in bioinspired composites," *Phys. Rev. E - Stat. Nonlinear, Soft Matter Phys.*, vol. 84, no. 1, pp. 1–4, 2011, doi: 10.1103/PhysRevE.84.015102.

[236] J. L. Liu, A. K. Singh, H. . Lee, T. E. Tay, and V. B. C. Tan, "The Response of Bio-inspired Helicoidal Laminates to Small Projectile Impact," *Int. J. Impact Eng.*, vol. 142, p. 103608, 2020, doi: 10.1016/j.ijimpeng.2020.103608.

[237] K. Karthikeyan, S. Kazemahvazi, and B. P. Russell, "Optimal fibre architecture of soft-matrix ballistic laminates," *Int. J. Impact Eng.*, vol. 88, pp. 227–237, Feb. 2016, doi: 10.1016/j.ijimpeng.2015.10.012.

[238] N. Suksangpanya, N. A. Yaraghi, D. Kisailus, and P. Zavattieri, "Twisting cracks in Bouligand

structures," *J. Mech. Behav. Biomed. Mater.*, vol. 76, pp. 38–57, 2017, doi: 10.1016/j.jmbbm.2017.06.010.

[239] M. Milwich, T. Speck, O. Speck, T. Stegmaier, and H. Planck, "Biomimetics and technical textiles: Solving engineering problems with the help of nature's wisdom," *Am. J. Bot.*, vol. 93, no. 10, pp. 1455–1465, 2006, doi: 10.3732/ajb.93.10.1455.